DIPLOMA THESIS

Integrable methods in gauge and string theories

József Konczer

Supervisor: Dr. Zoltán Bajnok
Senior research fellow
ELTE Institute for Theoretical Physics

Internal advisor: Dr. Péter Lévay
Research associate professor
BME Institute of Physics
Department of Theoretical Physics

BME
2013

Szakdolgozat kiírása

Maldacena sejtése szerint a maximálisan szuperszimmetrikus négydimenziós mértékelmélet ekvivalens egy tízdimenziós gravitációs elmélettel. Konkrétan az ötdimenziós anti de Sitter tér és az ötdimenziós gömb szorzatán mozgó szuperhúrok dinamikája – amely a kvantumgravitációt is magába foglalja – duális az ezen tér négydimenziós peremén keletkező mértékelmélettel. Ez a csodálatos dualitás erős-gyenge típusú, vagyis az erősen kölcsönható mértékelméletet klasszikus húrelméletre (gravitációra), míg az erősen kvantumos húr mozgását perturbatív mértékelméletre képzi le. A dualitás erős-gyenge jellege lehetőséget teremt az eddig elérhetetlen erősen csatolt mennyiségek kiszámolására, viszont lehetetlenné is teszi a két modell összehasonlítását és a sejtés ellenőrzését. Az előrelépést az jelentette, hogy mindkét modell integrálhatónak bizonyult abban a határesetben, melyben a színek számát végtelennek vesszük.

Önállósági nyilatkozat

Alulírott Konczer József, a Budapesti Műszaki és Gazdaságtudományi Egyetem hallgatója kijelentem, hogy dipomamunkámat a témavezetőm irányítása mellett önállóan, meg nem engedett segédeszközök nélkül készítettem. Amennyiben mások munkáját felhasználtam, azt mindig a forrás megjelölésével tettem.

Budapest, 2013. június 10.

.....
Konczer József

Köszönet nyilvánítás

Elsősorban szeretnék köszönetet nyilvánítani témavezetőmnek Bajnok Zoltánnak, akinek segítsége és szakmai tanácsai nélkül ez a munka nem születhetett volna meg.

Külön köszönöm Holló Lászlónak a sok-sok konzultációt és a sok emberi és szakmai támogatást. Takács Gábornak pedig köszönöm az inspiráló és kihívásokat mutató megjegyzéseit.

Végül de nem utolsó sorban szeretném megköszönni Csajbók Viktóriának, aki munkámban mindvégig szeretve támogatott.

Contents

1 Introduction

The electromagnetic, weak, strong and gravitational forces are the four fundamental interactions of Nature. The first two, unified by the electro-weak quantum field theory (QFT), have been tested with high accuracy. The strong interaction is formulated also as a QFT but its strongly coupled nature circumvented its precision tests, additionally, the gravitational interaction does not even have a satisfactory QFT formulation.

The gauge/gravity duality gives a hope to understand these two unsolved problems in one turn as it connects gauge theories with string theory (including gravity). This duality relates strongly coupled gauge theories to semi-classical string theory and the deeply quantum string theory (gravity) to perturbative gauge theory. The best chance to show the conjectured equivalence is the 't Hooft limit of the maximally supersymmetric 4D QFT as in this limit integrability of the 2D string theory shows up.

In the last twenty years, motivated by particle physics problems, there has been intensive research and relevant progress in 2D integrable QFTs. Integrable theories were solved in the bulk and also with boundaries by determining exactly the spectrum of particles together with their scattering data which were then used to calculate the full spectrum at any finite size [1].

1.1 Motivation

Two dimensional quantum field theories (2D QFTs) are relevant in various areas of physics. We use them as toy models to understand fundamental questions and develop new methods which we test in simplified circumstances. They have direct applications as well: In certain solid state systems the effective dimension of the physical space time can be smaller and a two dimensional description in many cases can provide a good approximation. Recent advances in the AdS/CFT correspondence, which relates string (gravity) theory on the Anti de Sitter background to 4D conformal gauge theory [19], showed that 2D integrable QFTs can describe both quantum gravity and 4D strongly coupled gauge theories. The exact solution of the correspondence gives a hope to understand these two unsolved problems of contemporary theoretical physics.

1.2 Background

The general strategy to solve 2D integrable field theories is the bootstrap method. It starts with the S-matrix bootstrap [31]. The scattering matrix, which connects asymptotic in and out states, is determined from its properties such as factorizability, unitarity, crossing symmetry and Yang-Baxter equation (YBE) supplemented by the maximal analyticity assumption. The next step is the form factor bootstrap [25] when matrix elements of local operators between asymptotic states are computed using their analyticity properties originating from the already computed S-matrix. Supposing maximal analyticity leads to a set of solutions each of which corresponds to a local operator of the theory. In the third step these form factors are used to build up the correlation (Wightman) functions via their spectral representation and describe the theory completely off mass shell in infinite volume.

The finite volume solution is considerably more difficult, even the spectral problem

requires much effort. This can be achieved by systematically taking into account the finite size effects due to the scatterings of particles. The leading finite size effect of a multiparticle state comes from the quantization of momenta which is dictated by the scattering matrix [17]. It incorporates all polynomial corrections in the inverse of the volume. In addition, there are exponentially small (Lüscher) corrections as well and their leading contributions come from the polarization of the sea of virtual particles [18]. For small volumes, these effects become dominant and one needs to perform a resummation of the virtual corrections, which sometimes can be carried out in the form of nonlinear integral equations [29].

1.3 Outline

To understand deeper, and to develop more accurate numerical methods for 2D QFTs in the present thesis the defect scaling Lee-Yang (LY) model is under scope. It is an integrable 2D QFT with a single defect line. The bulk theory is already well understood, and famous not just because of its simplicity. It was the first model where the truncated conformal space approach (TCSA) was developed and used with great accuracy. Due to the importance of boundary conditions and impurities in real physical systems it is natural to deal with the simplest models where exact solutions can be made. Despite of its simplicity the form factor bootstrap of the defect model was not fully closed.

In my thesis I could calculate previously unknown form factor candidates in the theory and numerically check their validity. Surprisingly the presence of the defect could help to avoid numerical difficulties in the standard TCSA method, and gave inspiration to improve it for other integrable models.

In section 2 I describe the bootstrap method for integrable models in infinite volume, demonstrated on the scaling and defect scaling LY model. To be able to compare these quantities with numerical calculations I describe the simplest finite volume corrections in section 3. This formalism is based on the description of finite volume spectrum provided by Bethe-Yang equations. In section 4 I introduce the conformal field theory, to explain the main building blocks of the defect scaling LY models UV description. After that in section 5 the TCSA method is presented. In the 6. section the defect scaling LY model is fully introduced in finite volume. I also summarize the previously achieved form factor bootstrap solutions here. Finally in section 7 I write down my analytical and numerical results.

In the whole thesis natural units are used, where $[c] = 1$ and $[\hbar] = 1$. [1]

2 Integrable models

In this section I try to give a brief introduction into quantum integrable systems and their special features.

In classical mechanics integrable systems are very special, because they can be solved by quadratures and we can find enough conserved quantities[2] (functions on the phase space) whose Poisson bracket is zero, and are functionally independent. Because of these

[1] In these units $[x] = [t] = m$, $[E] = [p] = [m] = m^{-1}$, and the action $[S] = 1$.

[2] for a Hamiltonian system with n dimensional configuration space n conserved quantities.

properties these systems have many special features, which helps us to analyze them in depth. Integrable models can be defined not just for systems with finite dimensional phase space, but also for classical field theories. One of the oldest nontrivial integrable model of this type is the sine-Gordon model in $1+1$ dimension (which is fortunately not just solvable, but have a number of applications).

It can be defined by the Lagrangian density:

$$\mathcal{L} = \frac{1}{2}(\partial_t \varphi)^2 - \frac{1}{2}(\partial_x \varphi)^2 - \frac{m^2}{b^2}(1 - \cos b\varphi), \tag{1}$$

where m is a mass term, as for small values of φ it gives back a free field with mass m, and b is an arbitrary parameter. [3] To simplify the further equations we can introduce the potential $V(\varphi) = \frac{m^2}{b^2}(1 - \cos b\varphi)$.

The theory can be defined in infinite or in finite volume. In the infinite case at every solution with finite energy φ goes to some integer times $2\pi/b$, while in the finite volume case we have to specify boundary conditions, for example periodic ones. First we consider the infinite volume case for simplicity.

It can be immediately seen, that the theory is relativistic invariant, so if we find time independent solutions, they can be boosted up to get new, time dependent ones.

In the sine-Gordon theory we can find infinitely many conserved charges which are space integrals of local quantities, and the solutions can be build up from well localized excitations called solitons, antisolitons, and breathers (what can be interpreted as a bound state of a soliton and an antisoliton).

To be explicit, here are the "standing" soliton, antisoliton and breather solutions:

$$\varphi_s(x,t) = \frac{4}{b} \arctan\left(e^{mx}\right), \tag{2}$$

$$\varphi_{\bar{s}}(x,t) = \frac{4}{b} \arctan\left(e^{-mx}\right), \tag{3}$$

$$\varphi_B(x,t) = \frac{4}{b} \arctan\left(\frac{\sin(mut\gamma')}{u\cosh(mx\gamma')}\right), \tag{4}$$

where u is a continuous parameter, and $\gamma' = \frac{1}{\sqrt{1+u^2}}$.

These solutions have well defined energies and momentum, which transforms covariantly for the Lorentz transformation. To describe the higher spin conserved quantities, it is more convenient to introduce the light cone coordinates:

$$x_\pm = \frac{1}{2}(t \pm x), \tag{5}$$

where the Lorentz transformation with velocity $v = \tanh\Lambda$ acts simpler:

$$x'_\pm = e^{\mp\Lambda} x_\pm \tag{6}$$

This notation helps us to write the energy and momentum conservation into a more general form, stating that a simply transforming so called spin ± 1 quantity is conserved:

[3] In the classical theory it it is not a relevant parameter, as it can be eliminated by rescaling the field, but in the quantum case it can change even the particle content of the theory.

$$Q_{\pm 1}[\varphi] = E[\varphi] \pm P[\varphi] = \int \left(\frac{1}{2}(\partial_{\pm}\varphi)^2 + V(\varphi) \right) \mathrm{d}x, \tag{7}$$

In general we will use a notation, where the Q_s charges transforms as: $Q'_s = e^{s\Lambda} Q_s$ under Lorentz transformation.

It can be shown, that if we build up a sine-Gordon solution from (finite number of) multi-particle states, then if we evaluate the solution at infinitely past, and at infinitely future, then we will find well separated solitons, which has the same shape, like the one particle solution in the vacuum. This solidness of these particles justify their name.

In classical theory we can discover one more interesting property. We can see the same set of particles in the far past and in the far future, but in the opposite order. In the past, the fastest (with sign) particle is the first, while in the future it is the last. ($1+1$ dimension is special because it make sense to order these particles.)

For the first sight this is plausible, but in non integrable theory even if there are some particle like solutions, particle creation and annihilation during collisions could happen. However integrability forbids these effects here.

Again because of the conserved higher spin quantities the particle collisions can be separated, it means that every 3 or even more particle collisions are just the sum of separated two particle collisions.

To be explicit again, I write down here a spin 3 conserved charge for the sine-Gordon theory:

$$Q_{\pm 3}[\varphi] = \int \left(\frac{1}{2b^2}(\partial_{\pm}^2\varphi)^2 - \frac{1}{8}(\partial_{\pm}\varphi)^4 + (\partial_{\pm}\varphi)^2 V(\varphi) \right) \mathrm{d}x \tag{8}$$

In the formula a general $V(\varphi)$ is written, but for its conservation it is crucial to have a potential satisfying the equation $V'' = \alpha V$ for some α.

As a consequence it is enough to investigate the two particle scatterings. The reason, why does this conservation property apply the factorization of scatterings, is more transparent in the quantum case.

A good quantity to characterise a scattering in $1+1$ dimension is the time shift. Time shift is the time difference between interaction and free motion. Positive time shift means an effective attraction, and negative repulsion.

If we calculated the time shifts for the particles in sine-Gordon model, we can see an effective repulsion between the same type of solitons, and an attraction between soliton and antisoliton. It now makes sense to interpret the breathers as some kind of bound states.

Many features of classical integrable field theories can be generalize into the quantum case. A relativistic quantum field theory is called integrable if one can find infinitely many commuting and functionally independent charges, which are space integrals of local operators.

If we have local fields in relativistic field theory (RFT), we have to determine how they transform under Lorentz transformation. It turns out, that these are typically higher spin quantities introduced previously. We say that a local field $\mathcal{O}$ has spin s if it transforms under Lorentz transformation as:

$$\mathcal{O}'(x') = e^{s\Lambda} \mathcal{O}(x) \tag{9}$$

If we can identify such quantities, we can factorize the many particle scatterings to two particle scatterings. Different factorizations results in the Yang-Baxter equations. It can be intuitively understood, if we build up for simplicity Gaussian wave packets, and we watch what happens, if we transform the system by a $e^{iQ_s t}$ operator which is a symmetry. As higher spin charges transform different momentum particles differently, the factorisation follows [11].

As for illustration the oldest known integrable relativistic quantum field theory, the sine-Gordon theory can be used. Here we have a Lagrangian set up what can be viewed as a perturbation of a massive Klein-Gordon theory, which can be treated by Feynman diagrams. It can be also viewed as the perturbation of a massless free boson, and used the language of conformal field theory, that will be introduced later in section 4. Finally because of integrability the so called bootstrap can be used, and compared for the previous views. The whole analysis can be found in [8] and [24].

2.1 S-matrix bootstrap

2.1.1 General S-matrix axioms

The first part of this subsection follows a very general and precise description of the topic in [11]. It will be more general, what would be needed for the following sections. Here I will summarize the S-matrix axioms for general N scalar fields ϕ_i with mass m_i. Its creation operators at momentum p is $a_i^\dagger(p)$ and higher spin charges act as

$$Q_s a_i^\dagger(0)\,|0\rangle = q_i^{(s)} a_i^\dagger(0)\,|0\rangle$$

In $1+1$ dimensional integrable models we have enough symmetry to construct the explicit forms of S-matrices, without calculating any Feynman diagrams, just by postulating some axioms for the structure of it.

In integrable RFTs where higher spin conserved quantities exists, we can see:

- no particle production;
- equality of the sets of initial and final momenta;
- factorisability of the $n \to n$ S-matrix into a product of $2 \to 2$ S-matrices.

In more than 2 dimensional theories it also simply implies that the S-matrix is trivial (we can shift any particle world lines to not to collide by higher spin generators (showed by Coleman and Mandula in 1967)), however in 2D, collisions will happen after any shift, and the S-matrix can have nontrivial phase and can mix particles with the same mass (for example soliton antisoliton mixing in the sine-Gordon theory is allowed).

That is why it is enough to completely determine the $2 \to 2$ S-matrices:

$$S_{ij}^{kl}(p_1, p_2; p_3, p_4) = {}_{out}\langle a_i(p_3) a_j(p_4) | a_k^\dagger(p_1) a_l^\dagger(p_2)\rangle_{in} \tag{10}$$

In RFT the S-matrix can be expressed in terms of the Mandelstam variables s, t and u:

$$s = (p_1{+}p_2)^2\ , \quad t = (p_1{-}p_3)^2\ , \quad u = (p_1{-}p_4)^2\ ,$$

with $s{+}t{+}u = \sum_{i=1}^4 m_i^2$. In $1+1$ dimensions only one of these is independent, and it is standard to focus on s, the square of the forward-channel momentum.

In terms of the rapidity difference $\theta_{12} = \theta_1 - \theta_2$,

$$s = m_i^2 + m_j^2 + 2m_i m_j \cosh\theta_{12} \ .$$

For a physical process, θ_{12} is real and so s is real and satisfies $s \geq (m_i+m_j)^2$. But we can consider the continuation of $S(s)$ into the complex plane. Placing the branch cuts in the traditional way, this results in a function with the following properties:
• S is a singlevalued, meromorphic function on the complex plane with cuts on the portions of the real axis $s \leq (m_i - m_j)^2$ and $s \geq (m_i+m_j)^2$. Physical values of $S(s)$ are found for s just above the right-hand cut. This first sheet of the full Riemann surface for S is called the physical sheet.
• S is real-analytic: it takes complex-conjugate values at complex-conjugate points:

$$S_{ij}^{kl}(s^*) = \left[S_{ij}^{kl}(s)\right]^* .$$

In particular $S(s)$ is real if s is real and $(m_i-m_j)^2 \leq s \leq (m_i+m_j)^2$.

To see explicitly this kind of continuation I show in advance the S-matrix of the scaling LY model, where there is just one particle with unite mass (here S is just a phase factor in physical processes)

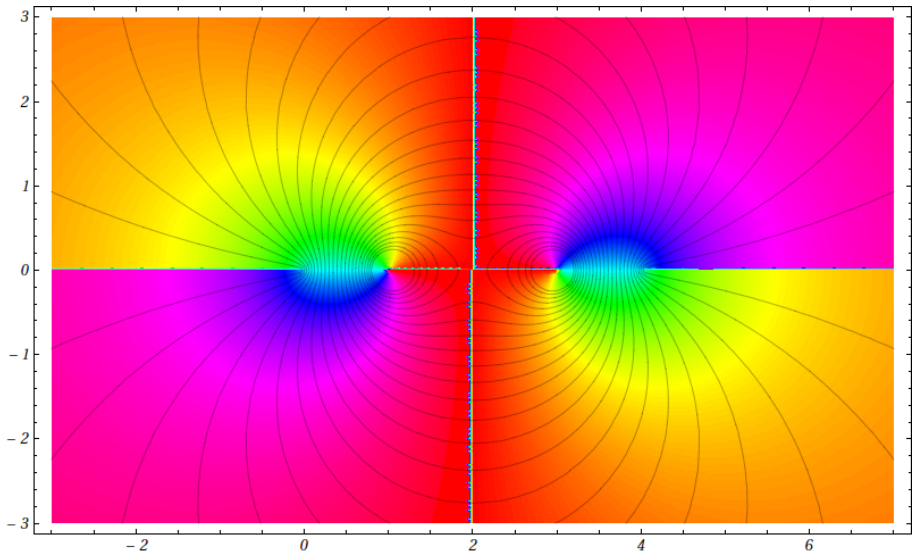

Figure 1: Analytic continued S of the LY theory in s variable

Where on the figure 1 the phase of the complex function is represented by the hue in standard hsb color scheme (●, ●, ●, ● represents 1, i, -1, $-i$ respectively), and the contour lines belongs to the logarithm of the absolute value of S. [4]

On the picture we can see two branch points in $4m^2$ and in 0, two branch cuts on $(-\infty, 0)$ and $(4m^2, \infty)$, and two first order poles between them.

It will be more comfortable to map this complex s plane into the difference of rapidities. For identical particles:

$$s = 2m^2(1 + \cosh(\theta_2 - \theta_1)), \tag{11}$$

[4]The cross in the middle is just numeric error because of the non continuity of phase between 0 and 2π

So we can use the map:

$$\theta_{12} = \cosh^{-1}(s/(2m^2) - 1) \tag{12}$$

From that we can explicitly see why is used $\mathbb{R} \times [0, i\pi]$ as the "physcal strip" for the difference of rapidities. We can see the same example on figure 2.

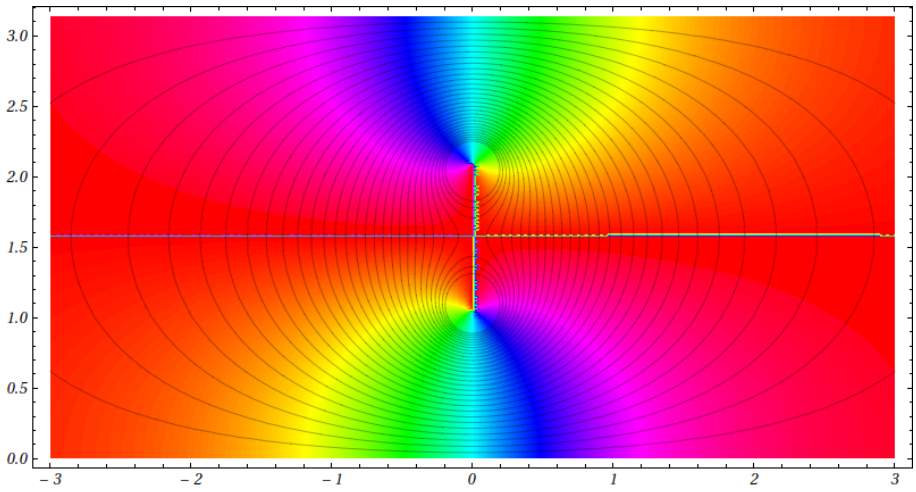

Figure 2: Analytic continued S of the LY theory in θ

To get the S matrix axioms in a compact way, I introduce here the Zamolodchikov-Faddeev (ZF) algebra:

In infinite volume it makes sense to define left and right directions. As we observed, in $t \to -\infty$ particles are far from each other, and the fastest is the leftmost. It can be formulated as:

$$A^+_{a_1}(\theta_1)A^+_{a_2}(\theta_2)\dots A^+_{a_n}(\theta_n)|0\rangle$$

with

$$\theta_1 > \theta_2 > \dots > \theta_n \ .$$

And at $t \to \infty$ the situation is similar, just now the fastest particle is the rightmost. In ZF language:

$$A^+_{b_1}(\theta_1)A^+_{b_2}(\theta_2)\dots A^+_{b_n}(\theta_n)|0\rangle$$

now with

$$\theta_1 < \theta_2 < \dots < \theta_n \ .$$

However this algebra is defined just for these two completely ordered sets of rapidities, we can extend it with the help of S-matrices and crossing.

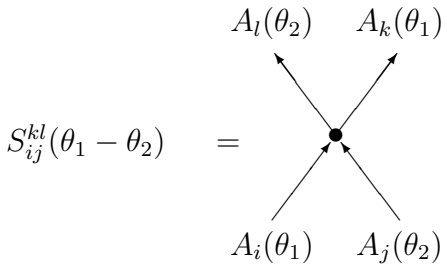

Figure 3: The two-particle S-matrix

$$A_i^+(\theta_1)\,A_j^+(\theta_2) = S_{ij}^{kl}(\theta_1-\theta_2)\,A_l^+(\theta_2)\,A_k^+(\theta_1)\,, \tag{13}$$

$$A_i(\theta_1)\,A_j(\theta_2) = S_{ij}^{kl}(\theta_1-\theta_2)\,A_l(\theta_2)\,A_k(\theta_1)\,, \tag{14}$$

$$A_i(\theta_1)\,A_j^+(\theta_2) = S_{ij}^{kl}(\theta_2-\theta_1)\,A_l^+(\theta_2)\,A_k(\theta_1) + 2\pi\delta_{ij}\delta(\theta_1-\theta_2)\,. \tag{15}$$

In this language the S-matrix axioms are the following:

• Unitarity: $S_{ij}^{nm}(\theta)S_{nm}^{kl}(-\theta) = \delta_i^k\delta_j^l$; [5]

• Crossing: $S_{ij}^{kl}(\theta) = S_{i\bar{l}}^{k\bar{j}}(i\pi-\theta)$; [6]

• Maximal analyticity: $S_{ij}^{kl}(\theta)$ is a meromorphic function of the rapidity on the physical strip having poles on the imaginary axis only. Each pole has to be explained as so called Coleman-Thun diagrams, bound state, or an anomalous threshold (in non integrable theory). The physical value of the scattering matrix is given by $\lim_{\epsilon\to 0^+} S_{ij}^{kl}(\theta+i\epsilon)$ for $\Re(\theta)>0$ and for the crossed process by $\lim_{\epsilon\to 0^+} S_{ij}^{kl}(\theta+i(\pi-\epsilon))$ for $\Re(\theta)<0$ [8];

• Yang-Baxter equations:

$$S_{ij}^{\beta\alpha}(\theta_{12})S_{\beta k}^{n\gamma}(\theta_{13})S_{\alpha\gamma}^{ml}(\theta_{23}) = S_{jk}^{\beta\gamma}(\theta_{23})S_{i\gamma}^{\alpha l}(\theta_{13})S_{\alpha\beta}^{nm}(\theta_{12})\ ,$$

where $\theta_{ab}=\theta_a-\theta_b$, and θ_1, θ_2 and θ_3 are the rapidities of particles i, j and k.

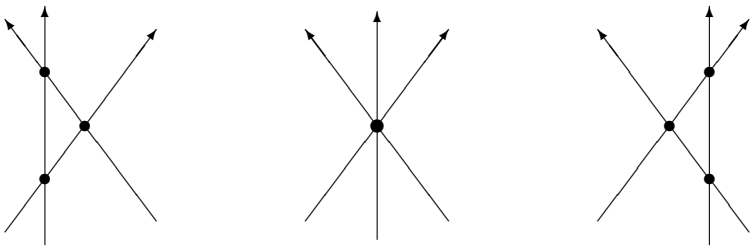

(1) (2) (3)

Figure 4: Illustration of Yang-Baxter equations

As mentioned poles have a special meaning. Naively in integrable theory these must be bound states, but it turns out that so called Coleman-Thun diagrams can be drawn in the perturbative language. Especially in 2D they can appear at some complex rapidity differences as poles (in higher dimensions these would be branch points). These diagrams

[5] as the consequence of the algebra, and the single-valued nature of products of the non-commuting symbols.

[6] $\bar{j}$ labels the jth antiparticle.

are special, because at some incoming (complex) rapidities the internal lines are on shell. For illustration an example from the sine-Gordon theory:

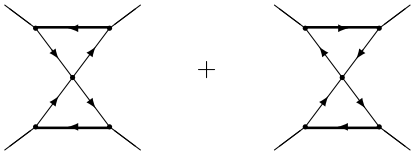

Figure 5: Coleman-Thun diagram of breathers

If we can find $S_{ij}^{kl}(\theta)$ for every kind of particles in the theory, and we can explain every pole as a creation of particles or a Coleman-Thun diagram, then the bootstrap is closed, and we completely solved the scattering theory of the model.

2.1.2 Bootstrap of the scaling LY model

Now we can try to find the simplest integrable theories, defined just by its particle content and scattering matrix.

The most trivial example of a complete bootstrap is $S(\theta) \equiv 1$. This actually describes the free boson.

Now lets find some more complicated one following [8]: Let have first just one particle in the theory (which is its own antiparticle), then the S-matrix is a function. Let it be $S(\theta) = f(\theta)/f(-\theta)$. In this case the unitarity is automatically satisfied. To satisfy crossing, we introduce the variable $x = e^{\theta}$. If we make a crossing, it changes as: $x(i\pi - \theta) = -e^{-\theta} = -x(\theta)^{-1}$. Consequently if $f(x)$ is invariant under this change, then the crossing is satisfied also. The simplest example for this kind of function is $f(x) = x - x^{-1} + a$

Now we have the following guess for the S-matrix:

$$S(\theta) = \frac{\sinh(\theta) - a}{\sinh(\theta) + a} \tag{16}$$

To have a unitary S-matrix, a should be purely imaginary, and to satisfy the maximal analyticity (so avoid poles outside the imaginary line) $|a| \leq 1$. As a consequence we can choose an $\alpha \in (0, 2\pi)$ [7], to have:

$$S(\theta) = \frac{\sinh(\theta) + i\sin(\alpha)}{\sinh(\theta) - i\sin(\alpha)} \tag{17}$$

Now the S-matrix has poles at $\theta \in \{i\alpha, i(\pi - \alpha)\}$. We can not introduce a Coleman-Thun diagram for this situation, so we have to stand that we found a bound state, whit mass: $m_2 = 2m\cos(\alpha/2)$. This immediately explains the second pole as a crossed channel process. Now we force to have just one type of particle in the theory, so we demand to satisfy $m_2 = m$.

To have the pole really on the physical strip, there is just one solution, namely the $\alpha = \frac{\pi}{3}$, what defines the scaling LY model with S-matrix:

[7] $\alpha = 0$ results the already mentioned $S(\theta) \equiv 1$ case.

$$S(\theta) = \frac{\sinh\theta + i\sin\frac{\pi}{3}}{\sinh\theta - i\sin\frac{\pi}{3}}, \tag{18}$$

Which satisfies the fusion property:

$$S(\theta) = S(\theta + i\frac{\pi}{3})S(\theta - i\frac{\pi}{3}) \tag{19}$$

The two diagrams which explain the poles on figure 2 are the following:

Figure 6: Diagrams in scaling LY model representing the poles

2.2 T-matrix bootstrap

The S-matrix bootstrap was successfully closed for many types of integrable QFTs. This is a language which can be used basically in the infinite volume case, but can be extended with the help of Bethe-Yang equations or more precise thermodynamical Bethe anzats (TBA) to finite volume with periodic boundary conditions. However in statistical physics, or in condensed matter physics boundary conditions are usually different. It motivates to extend the method for other boundary conditions. We can try to find some boundary conditions, which do not break the integrability, and where the (reflection) R-matrix bootstrap can be defined and solved. This bootstrap was successfully closed [13] and gave a good starting point to analyze defect theories.

Boundary conditions can be also viewed as a system with localized defect(s). In Hamiltonian formalism it means, that we add a new operator to the theory localized to some definite place(s).

Analyzing defects in the theory is also good for better understanding of the previous model, and to widen the range of possible applications.

If we introduce a defect, which preserves integrability, then we have to be able to calculate its transmission (T) and reflection (R) matrices.

It turns out, that these integrability preserving defects imply (if $S \neq \pm 1$) that they are purely transmissive, or purely reflective [9]. The two cases seems to be absolutely different, but in [4] was shown that there is a connection between them.

In this section I will summarize the main steps of the T-matrix bootstrap illustrated on the defect scaling LY model based on [15] and [7].

If we think in spacetime coordinates, we can interpret the defect as an $x = const$ line. It does not brake the time shifting invariance, so the energy of the system should be conserved. However it breaks the translational symmetry, so the momentum conservation could be broken. However it turns out, that by introducing a defect momentum, the whole momentum of a state will be conserved. It implies, that these integrability preserving defects are topological, i.e. their position can be freely changed, without effecting the theory (if we take care on topology).

In the fusing method used in [7] the already known reflection matrices were used to construct a one parameter family of transmission matrices.

The transmission matrices can be split into two parts, $T_-(\theta)$ for $\theta > 0$ and $T_+(-\theta)$ for $\theta < 0$. In this notation we can introduce the unitarity and crossing symmetries for the transmission matrices [4]:

$$T_+(-\theta) = T_-^{-1}(\theta) \quad ; \qquad T_-(\theta) = T_+(i\pi - \theta)\,. \tag{20}$$

The S-matrix of the scaling LY model is already known, and here we introduce a more helpful notation:

$$S(\theta) = \frac{\sinh\theta + i\sin\frac{\pi}{3}}{\sinh\theta - i\sin\frac{\pi}{3}} = -\left(\frac{1}{3}\right)\left(\frac{2}{3}\right) \ , \qquad (x) = \frac{\sinh\left(\frac{\theta}{2} + \frac{i\pi x}{2}\right)}{\sinh\left(\frac{\theta}{2} - \frac{i\pi}{2}\right)}.$$

Because of the fusion property of the theory (19), the T-matrices satisfy also the bootstrap equations:

$$T_-\left(\theta + \frac{i\pi}{3}\right) T_-\left(\theta - \frac{i\pi}{3}\right) = T_-(\theta)\,. \tag{21}$$

These last two equations with unitarity and crossing property determine the T-matrix:

$$T_- = [b+1]\,[b-1] \ ; \qquad T_+ = [5-b]\,[-5-b] \ ; \qquad [x] = i\frac{\sinh\left(\frac{\theta}{2} + i\frac{\pi x}{12}\right)}{\sinh\left(\frac{\theta}{2} + i\frac{\pi x}{12} - i\frac{\pi}{2}\right)}. \tag{22}$$

In the case of one defect line in the theory, the unitarity of the T-matrix forces the parameter to be $b = \pm 3 + i\alpha$ with $\alpha \in \mathbb{R}$ (if we put two defects they can be more general). In this case the followings are also true:

$$T_+(\theta)T_-(-\theta) = 1; \quad T_-(\theta) = T_+(i\pi - \theta) \tag{23}$$

2.3 The form factor bootstrap

To completely describe a quantum field theory, we have to be able to calculate any n point functions of any operators, appearing in the theory, as these can be used to calculate physical quantities, like correlation functions, or responses. Furthermore according to the LSZ reduction formulas, from these information we can completely recover the Hilbert space, and the forms of the operators in the theory, therefore this is a unique characterization of the analyzed model.

Traditionally it could be also done in a perturbative way (in a theory defined by Lagrangian density), but in $1+1$ dimensional integrable systems the axiomatic structure of the form factors (FF) is fruitful again. It is possible to write down abstractly all possible form factors appearing in a theory (defined by its particle content and S-matrix). After the classification of functional forms of possible form factors, the second task is to identify them, and make a match between FF candidates and local operators in the theory. This matching is in some cases still not proved, but we will use numerical investigations, to verify that in some way the simplest choices of form factor candidates can be used to described naturally appearing operators especially in the defect scaling Lee-Yang model.

In the first part I summarize the FF axioms for a $1+1$ dimensional integrable defect theory which contains only one particle, using the introduced ZF algebra. The subsection is based on [3] and [2].

2.3.1 The ZF algebra for defects

Once defects are introduced we have to make a distinction whether the particle arrives from the left (A) or from the right (B) to the defect. These particles can be even different from each other as they live in different subsystems. A multiparticle state is then described by

$$|\theta_1,\dots,\theta_n;\theta_{n+1},\dots,\theta_m\rangle = A^+(\theta_1)\dots A^+(\theta_n)D^+B^+(\theta_{n+1})\dots B^+(\theta_m)|0\rangle, \qquad (24)$$

where the ZF operators B^+ create particles on the right of the defect and satisfy similar defining relations to (14) with a possibly different scattering matrix. Yet, for simplicity, we restrict our discussion to the case when the two subsystems are identical with the same scattering matrix. Observe however, that this does not imply space parity invariance, since the defect may break it. In the initial state rapidities are ordered as $\theta_1 > \dots > \theta_n > 0 > \theta_{n+1} > \dots > \theta_m$. The final state, in which all scatterings and transmissions are already terminated, can be expressed in terms of the initial state via the multiparticle transmission matrix.

$$|\theta_1,\dots,\theta_n;\theta_{n+1},\dots,\theta_m\rangle = \prod_{i<j} S(\theta_i-\theta_j)\prod_{i=1}^{n} T_-(\theta_i)\prod_{i=n+1}^{m} T_+(-\theta_i)|\theta_m,\dots,\theta_{n+1};\theta_n,\dots,\theta_1\rangle \qquad (25)$$

Due to integrability it factorizes into pairwise scatterings and individual transmissions: $T_-(\theta)$ and $T_+(-\theta)$. We parametrize T_+ such a way that for its physical domain ($\theta<0$) its argument is always positive. Transmission factors satisfy unitarity and defect crossing symmetry (23).

The multiparticle transition amplitude can be derived by introducing the defect operator D^+ and the following relations in the ZF algebra:

$$A^+(\theta)D^+ = T_-(\theta)D^+B^+(\theta) \qquad ; \quad D^+B^+(-\theta) = T_+(\theta)A^+(-\theta)D^+ \qquad (26)$$

A defect is parity symmetric if $T_-(\theta)=T_+(\theta)$. Clearly $A^+(\theta=0)$ satisfies the properties of D^+ with $T_-(\theta)=S(\theta)=T_+(\theta)$. Thus a standing particle can be considered as the prototype of a parity symmetric defect. [8]

2.3.2 Coordinate dependence of the form factors

The form factor of a local operator $\mathcal{O}(x,t)$ is its matrix element between asymptotic states:

$$\langle\theta'_{m'},\dots,\theta'_{n'+1};\theta'_{n'},\dots,\theta'_1|\mathcal{O}(x,t)|\theta_1,\dots,\theta_n;\theta_{n+1},\dots,\theta_m\rangle,$$

[8] In the LY case $b=\pm 3$ results parity symmetry.

where in the presence of defects we have to distinguish if particles arrive from the left or from the right. In an initial state the rapidities are ordered as

$$\theta_1 > \cdots > \theta_n > 0 > \theta_{n+1} > \cdots > \theta_m$$

while in the final state oppositely. The adjoint state is defined to be on the language of ZF algebra:

$$\langle \theta'_{m'}, \dots, \theta'_{n'+1}; \theta'_{n'}, \dots, \theta'_1| = \langle 0|B(\theta'_{m'}) \dots B(\theta'_{n'+1}) D A(\theta'_{n'}) \dots A(\theta'_1) \tag{27}$$

Strictly speaking the form factor is defined only for initial/final states (i.e. for decreasingly/increasingly ordered arguments) but using the ZF algebra we can generalize them for any values and orders of the rapidities (and not just on the physical strip [25]).

The multiparticle asymptotic states are eigenstates of the conserved energy. This fact can be formulated in the language of the ZF algebra as

$$[H, A^+(\theta)] = m \cosh\theta \, A^+(\theta) \qquad ; \qquad [H, D^+] = e_D D^+ \tag{28}$$

In the second equation we supposed that the vacuum containing the defect has energy e_D. Classical considerations together with the topological nature of the defect suggest the existence of a conserved momentum with properties

$$[P, A^+(\theta)] = m \sinh\theta \, A^+(\theta) \qquad ; \qquad [P, D^+] = p_D D^+ \tag{29}$$

Thus, opposed to a general boundary theory, the defect breaks translation invariance by having a nonzero momentum eigenvalue p_D and not by destroying the existence of the momentum itself. As a consequence the time and space dependence of the form factor can be obtained as

$$\begin{aligned} &\langle \theta'_{m'}, \dots, \theta'_{n'+1}; \theta'_{n'}, \dots, \theta'_1 | \mathcal{O}(x,t) | \theta_1, \dots, \theta_n; \theta_{n+1}, \dots, \theta_m \rangle = \\ &\qquad e^{it\Delta E - ix\Delta P} F^{\mathcal{O}_\pm}_{(n',m')(n,m)}(\theta'_{n'+m'}, ..., \theta'_{n'+1}; \theta'_{n'}, ..., \theta'_1 | \theta_1, \dots, \theta_n; \theta_{n+1}, ..., \theta_{n+m}) \end{aligned} \tag{30}$$

with $\Delta E = m(\sum_j \cosh\theta_j - \sum_{j'} \cosh\theta'_{j'})$ and $\Delta P = m(\sum_j \sinh\theta_j - \sum_{j'} \sinh\theta'_{j'})$, and we distinguished if the operator was localized on the left, $\mathcal{O}_-$, or on the right, $\mathcal{O}_+$, of the defect as they might not be continous there. Same apply for operators localized at the defect ($x = 0$).

2.3.3 Crossing transformation of any of the form factors

The properties and analytical structure of the form factor $F_{(n'm'),(nm)}$ can be derived via the reduction formula from the correlation functions similarly to the boundary case [6]. Instead of going to the details of the calculation of [6] we note that all equations follow from the defining relations of the ZF algebra and the locality of the operator $[\mathcal{O}(0,0), A^+(\theta)] = 0$ except the crossing relation. This missing relation reads as

$$\begin{aligned} &F^{\mathcal{O}}_{(n\prime,m\prime)(n,m)}(\theta'_{n\prime+m\prime}, ..., \theta'_{n\prime+1}; \theta'_{n\prime}, ..., \theta'_1 | \theta_1, \dots, \theta_n; \theta_{n+1}, ..., \theta_{n+m}) = \\ &F^{\mathcal{O}}_{(n\prime,m\prime+1)(n,m-1)}(\theta_{n+m} + i\pi, \theta'_{n\prime+m\prime}, ..., \theta'_{n\prime+1}; \theta'_{n\prime}, ..., \theta'_1 | \theta_1, \dots, \theta_n; \theta_{n+1}, ..., \theta_{n+m-1}) \end{aligned} \tag{31}$$

By analyzing the crossing equation of the particle A^+ instead of B^+ we obtain

$$F^{\mathcal{O}}_{(n\prime,m\prime)(n,m)}(\theta'_{n\prime+m\prime},...,\theta'_{n\prime+1};\theta'_{n\prime},...,\theta'_1|\theta_1,\dots,\theta_n;\theta_{n+1},...,\theta_{n+m}) \quad = \\ F^{\mathcal{O}}_{(n\prime+1,m\prime)(n-1,m)}(\theta'_{n\prime+m\prime},...,\theta'_{n\prime+1};\theta'_{n\prime},...,\theta'_1,\theta_1-i\pi|\theta_2,\dots,\theta_n;\theta_{n+1},...,\theta_{n+m}) \tag{32}$$

Using any of the crossing equations above we can express all form factors in terms of the one-sided form factors:

$$F^{\mathcal{O}}_{(n,m)}(\theta_1,\dots,\theta_n;\theta_{n+1},...,\theta_{n+m}) := F^{\mathcal{O}}_{(0,0)(n,m)}(;|\theta_1,\dots,\theta_n;\theta_{n+1},...,\theta_{n+m}) \tag{33}$$

on which we focus in the followings.

The properties of this form factor follows from the ZF algebra relations and from the crossing relations and we postulate them in the next subsection as axioms.

2.3.4 Defect form factor axioms

The matrix elements of local operators satisfy the following axioms:

I. Transmission:

$$F^{\mathcal{O}}_{(n,m)}(\theta_1,\dots,\theta_n;\theta_{n+1},...,\theta_{n+m}) = T_-(\theta_n)F^{\mathcal{O}}_{(n-1,m+1)}(\theta_1,\dots,\theta_{n-1};\theta_n,\theta_{n+1},...,\theta_{n+m}) \tag{34}$$

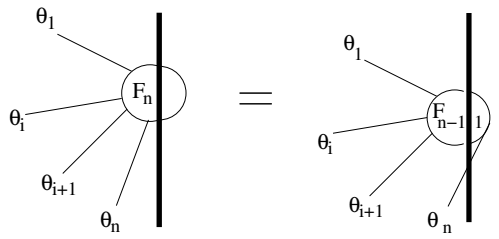

By means of this axiom we can express every form factor in terms of the *elementary* one

$$F^{\mathcal{O}}_n(\theta_1,\dots,\theta_n) = F^{\mathcal{O}}_{(n,0)}(\theta_1,\dots,\theta_n;) \tag{35}$$

It satisfies the further axioms:

II. Permutation:

$$F^{\mathcal{O}}_n(\theta_1,\dots\theta_i,\theta_{i+1},\dots,\theta_n) = S(\theta_i-\theta_{i+1})F^{\mathcal{O}}_n(\theta_1,\dots\theta_{i+1},\theta_i,\dots,\theta_n) \tag{36}$$

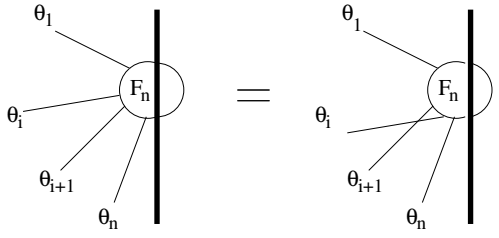

III. Periodicity:

$$F_n^{\mathcal{O}}(\theta_1, \theta_2, \dots, \theta_n) = F_n^{\mathcal{O}}(\theta_2, \dots \theta_n, \dots, \theta_1 - 2i\pi) \tag{37}$$

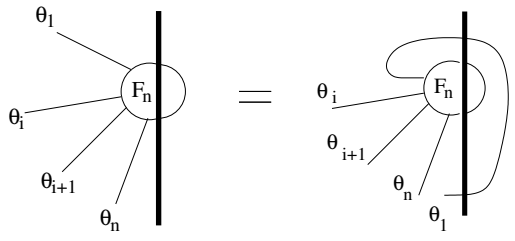

The physical singularities can be formulated as follows.

IV. Kinematical singularity:

$$-i\mathrm{Res}_{\theta=\theta\prime} F_{n+2}^{\mathcal{O}}(\theta + i\pi, \theta', \theta_1, ..., \theta_n) = \left(1 - \prod_{j=1}^{n} S(\theta - \theta_j)\right) F_n^{\mathcal{O}}(\theta_1, ..., \theta_n) \tag{38}$$

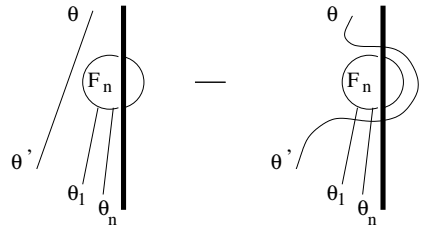

V. Dynamical bulk singularity [9] :

$$-i\mathrm{Res}_{\theta'=\theta} F_{n+2}^{\mathcal{O}}(\theta' + \frac{i\pi}{3}, \theta - \frac{i\pi}{3}, \theta_1, \dots, \theta_n) = \Gamma F_{n+1}^{\mathcal{O}}(\theta, \theta_1, \dots, \theta_n) \tag{39}$$

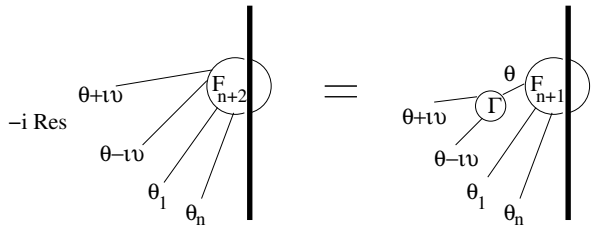

where Γ is the 3 particle on-shell coupling defined in (41).

VI. Dynamical defect singularity:

$$-i\mathrm{Res}_{\theta=iu} F_{n+1}^{\mathcal{O}}(\theta_1, \dots, \theta_n, \theta) = ig\tilde{F}_n^{\mathcal{O}}(\theta_1, \dots, \theta_n) \tag{40}$$

[9] for the scaling LY case

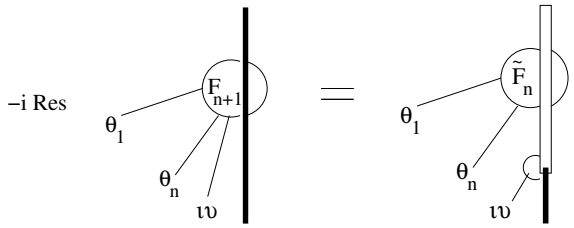

where g is the defect bound-state coupling.

The explicit definitions of Γ and g are:

$$S(\theta)|_{\theta\approx i\frac{2\pi}{3}} = -i\frac{\Gamma^2}{\theta - i\frac{2\pi}{3}} + \dots \tag{41}$$

$$T_-(\theta)|_{\theta\approx i\nu} = -i\frac{g^2}{\theta - i\nu} + \dots \tag{42}$$

A few remarks on the axioms:

Although the axioms (II, III, IV, V) look the same as the form factor axioms without the defect they are valid only for particles coming from the left. For any particle coming from the right one has to include a transmission factor, (axiom I). As a consequence the form factor of a bulk operator localized on the left of the defect, $\mathcal{O}_-$, is simply its bulk form factor

$$F_n^{\mathcal{O}_-}(\theta_1, \dots, \theta_n) = B_n^{\mathcal{O}}(\theta_1, \dots, \theta_n) \tag{43}$$

but when the same operator is localized on the right of the defect, $\mathcal{O}_+$, it is

$$F_n^{\mathcal{O}_+}(\theta_1, \dots, \theta_n) = \prod_i T_-(\theta_i) B_n^{\mathcal{O}}(\theta_1, \dots, \theta_n) \tag{44}$$

These apply for the left/right limits of the bulk fields at the defect as well.

2.3.5 Form factors of the defect scaling LY model

The bulk form factors for the scaling LY model are already determined [30] so we focus now on form factors of defect operators. In general, the solution compatible with the form factor axioms takes the form

$$F_n^{\mathcal{O}}(\theta_1, \dots, \theta_n) = \langle \mathcal{O} \rangle H_n \prod_i d(\theta_i) \prod_{i<j} \frac{f(\theta_i - \theta_j)}{x_i + x_j} Q_n(x_1, \dots, x_n) \tag{45}$$

where $f(\theta)$ is the minimal bulk two particle form factor, which satisfies:

$$f(\theta) = S(\theta) f(-\theta) \quad ; \qquad f(i\pi - \theta) = f(i\pi + \theta) \tag{46}$$

It can be written as:

$$f(\theta) = \frac{x + x^{-1} - 2}{x + x^{-1} + 1}\, v(i\pi - \theta)\, v(-i\pi + \theta), \tag{47}$$

where

$$\log v(\theta) = 2 \int_0^\infty \frac{dt}{t} e^{\frac{i\theta t}{\pi}} \frac{\sinh\frac{t}{2} \sinh\frac{t}{3} \sinh\frac{t}{6}}{\sinh^2 t} \tag{48}$$

This form automatically includes the pole of the dynamical singularity.

The one particle minimal defect form factor $d(\theta)$ is responsible for defect bound-states, and has the form:

$$d(\theta) = \frac{1}{4\sinh(\frac{\theta}{2} + \frac{i\pi}{12}(b-5))\sinh(\frac{\theta}{2} + \frac{i\pi}{12}(b-7))} = \frac{1}{\sqrt{3} + 2\cos(\frac{b\pi}{6} - i\theta)} = \frac{1}{\sqrt{3} + x\nu + x^{-1}\bar{\nu}} \tag{49}$$

where we introduced $\nu = e^{i\frac{\pi b}{6}}$ and $\bar{\nu} = \nu^{-1}$.

H_n is a normalization constant:

$$H_n = -\frac{\pi m^2}{4\sqrt{3}} \left(\frac{3^{\frac{1}{4}}}{2^{\frac{1}{2}} v(0)} \right)^n \quad . \tag{50}$$

$\langle \mathcal{O} \rangle$ is the vacuum expectation value of the operator.

Finally Q_n is a symmteric polynomial in its arguments $x_i = e^{\theta_i}$. The singularity axioms provide recursion relations between the polynomials Q_n as

$$\begin{aligned} Q_{n+2}(-x, x, x_1, ..., x_n) &= K_n(x, x_1, ..., x_n) Q_n(x_1, ..., x_n) & (51) \\ Q_{n+1}(x\omega, x\bar{\omega}, x_1, ..., x_{n-1}) &= D_n(x, x_1, ..., x_{n-1}) Q_n(x, x_1, ..., x_{n-1}) & (52) \end{aligned}$$

where $\omega = e^{\frac{i\pi}{3}}$, $\bar{\omega} = \omega^{-1}$ and we explicitly have

$$\begin{aligned} K_n(x, x_1, ..., x_n) &= (-1)^{n+1}(x^2\nu^2 - 1 + x^{-2}\nu^{-2}) & (53) \\ & \frac{x}{2(\omega - \bar{\omega})} \left(\prod_{i=1}^{n} (x\omega + x_i\bar{\omega})(x\bar{\omega} - x_i\omega) - \prod_{i=1}^{n} (x\omega - x_i\bar{\omega})(x\bar{\omega} + x_i\omega) \right) \end{aligned}$$

and

$$D_n(x, x_1, ..., x_{n-1}) = (\nu x + \nu^{-1}x^{-1}) x \prod_{i=1}^{n-1} (x + x_i) \tag{54}$$

Since $Q_n(x_1, ..., x_n)$ is a symmetric polynomial we use the elementary symmetric polynomials $\sigma_k^{(n)}(x_1, ..., x_n)$ defined by the generating function:

$$\prod_{i=1}^{n} (x + x_i) = \sum_{k=0}^{n} x^{n-k} \sigma_k^{(n)}(x_1, ..., x_n)$$

to formulate the already known results in section 6.2 and recently calculated ones in section 7.

3 States and form factors in finite volume

To verify the predictions made by the defect form factor bootstrap one can use the finite volume form factor formalism developed by Pozsgay and Takács [22][23]. Based on the description of the finite volume spectrum provided by the Bethe-Yang equations, the formalism gives all finite volume corrections that decay as a power in the inverse volume. The remaining corrections are suppressed exponentially as the volume increases. Here we confine ourselves to the power corrections, as these are sufficient to verify the validity of the defect form factor bootstrap.

3.1 Finite volume energy levels

The finite volume energy levels can be identified with multi-particle states $|\{I_1, \dots, I_n\}\rangle_L$ [10] containing n particles, labeled by quantum numbers $I_1, \dots, I_n$ which parametrize the quantization of particle momenta. The quantization conditions satisfied by the particle rapidities θ_k are the Bethe-Yang equations [5]

$$e^{imL\sinh\theta_k} T_-(\theta_k) \prod_{j\neq k} S(\theta_k - \theta_j) = 1 \qquad k = 1, \dots, n \tag{55}$$

Taking the logarithm, these equations can be rewritten as

$$Q_k(\theta_1, \dots, \theta_n)_L = 2\pi I_k \qquad k = 1, \dots, n \tag{56}$$

where

$$Q_k(\theta_1, \dots, \theta_n) = mL\sinh\theta_k - i\log T_-(\theta_k) - \sum_{j\neq k} i\log S(\theta_k - \theta_j). \tag{57}$$

(We chose the cut of the complex logarithm to be smooth on the whole interval, and we set $\log(-1) = \pi$.)

The energy is given by

$$E(L) = E_0(L) + \sum_{k=1}^{n} m\cosh\theta_k + O(e^{-\mu L}) \tag{58}$$

where μ is some characteristic scale, and $E_0(L)$ is the ground state (vacuum) energy.

The kth equation in (56) characterizes the monodromy of the wave functions under moving the kth particle to the right and around the circle; in doing so, one picks up the phase from crossing the defect, the scattering with the other particles (note the order of the rapidity difference inside S, which corresponds to particle k entering the scattering from the left), and the plane wave. The reason why only $T_-(\theta)$ enters is that it is the phase-shift suffered a particle of $\theta > 0$ when crossing the defect from the right; on the other hand, if a given particle has $\theta < 0$ its monodromy when crossing from the right to the left would be given by $T_+(-\theta)$. Therefore, when crossing from the left to the right the phase-shift is given by

$$T_+(-\theta)^{-1}$$

which is equal to $T_-(\theta)$ by defect unitarity. As a result, eqn. (56) describe all states in the spectrum by letting the sign of the rapidities free, i.e. by letting I_k to take any integer values. However, due to $S(0) = -1$ the multi-particle wave-functions are non-vanishing only if all the rapidities, and therefore all the quantum numbers, take distinct values [29].

This can be understood as these particles would behave at small rapidity differences as fermions.

The density of states in finite volume can be obtained from the Jacobi determinant of the mapping provided by the Q_k from rapidity space to the space of the quantum numbers:

$$\rho_n(\theta_1, \dots, \theta_n)_L = \det\left\{\frac{\partial Q_k(\theta_1, \dots, \theta_n)_L}{\partial\theta_j}\right\}_{k,j=1,\dots,n} \tag{59}$$

[10] $|\underline{n}\rangle$ in section 7.

3.2 Non-diagonal matrix elements

Using the arguments in the work [22], the absolute value of finite volume matrix elements of a defect operator can be obtained from

$$|\langle\{J_1,\dots,J_n\}|\,\mathcal{O}\,(t=0)\,|\{I_1,\dots,I_k\}\rangle_L| = \left|\frac{F^{\mathcal{O}}\left(\tilde{\theta}'_n+i\pi,\dots,\tilde{\theta}'_1+i\pi,\tilde{\theta}_1,\dots,\tilde{\theta}_k\right)}{\sqrt{\rho_n\left(\tilde{\theta}'_1,\dots,\tilde{\theta}'_n\right)_L\,\rho_k\left(\tilde{\theta}_1,\dots,\tilde{\theta}_k\right)_L}}\right|+O\left(e^{-\mu L}\right) \tag{60}$$

where $F^{\mathcal{O}}$ is the infinite volume form factor, $\tilde{\theta}_1,\dots,\tilde{\theta}_k$ and $\tilde{\theta}'_1,\dots,\tilde{\theta}'_n$ are the solutions to the Bethe-Yang equation (56) with quantum numbers $I_1,\dots,I_k$ and $J_1,\dots,J_n$, respectively.

3.3 Diagonal matrix elements

Formula (60) is valid if there are no disconnected terms in the matrix element. Disconnected terms arise when there is at least one rapidity value among the $\tilde{\theta}_1,\dots,\tilde{\theta}_m$ which coincides with a value occurring in $\tilde{\theta}'_1,\dots,\tilde{\theta}'_n$. Following two energy levels as the volume L varies, this can occur at particular isolated values of L, but these cases are not interesting as the matrix element can be evaluated by taking the limit of (60) in the volume. Therefore the only interesting cases are when disconnected terms are present for a continuous range of the volume L. Due to the presence of interactions (the S terms) in (56) this can only occur in very specific situations; the only generic class is when the matrix element is diagonal, i.e. the two states are eventually identical, in which case disconnected terms are present for all values of L.

In this case, we can proceed by analogy to the bulk and boundary cases. For diagonal matrix elements

$$\langle\{I_1,\dots,I_n\}|\mathcal{O}|\{I_1,\dots,I_n\}\rangle_L$$

(60) shows that the relevant form factor expression is

$$F^{\mathcal{O}}(\theta_n+i\pi,...,\theta_1+i\pi,\theta_1,...,\theta_n)$$

Due to the existence of kinematical poles this must be regularized; however the end result depends on the direction of the limit. The terms that are relevant in the limit can be written in the following general form:

$$\begin{aligned} &F^{\mathcal{O}}(\theta_n+i\pi+\epsilon_n,...,\theta_1+i\pi+\epsilon_1,\theta_1,...,\theta_n) = \\ &\prod_{i=1}^{n}\frac{1}{\epsilon_i}\cdot\sum_{i_1=1}^{n}...\sum_{i_n=1}^{n}\mathcal{A}_{i_1...i_n}(\theta_1,\dots,\theta_n)\epsilon_{i_1}\epsilon_{i_2}...\epsilon_{i_n}+\dots \end{aligned} \tag{61}$$

where $\mathcal{A}^{a_1\dots a_n}_{i_1\dots i_n}$ is a completely symmetric tensor of rank n in the indices $i_1,\dots,i_n$, and the ellipsis denote terms that vanish when taking $\epsilon_i\to 0$ simultaneously.

The connected matrix element can be identified as the ϵ_i independent part of eqn. (61), i.e. the part which does not diverge whenever any of the ϵ_i is taken to zero:

$$F^{\mathcal{O}}_{conn}(\theta_1,\theta_2,...,\theta_n) = n!\,\mathcal{A}_{1\dots n}(\theta_1,\dots,\theta_n) \tag{62}$$

where the appearance of the factor $n!$ is simply due to the permutations of the ϵ_i.

Following [22] and [16], we are lead to the following expression [11]

$$\langle\{I_1\dots I_n\}|\mathcal{O}|\{I_1\dots I_n\}\rangle_L = \\ \frac{1}{\rho_n(\tilde{\theta}_1,\dots,\tilde{\theta}_n)_L}\sum_{A\subset\{1,2,\dots n\}}(-1)^{|A|}F^{\mathcal{O}}_{conn}(\{\tilde{\theta}_k\}_{k\in A})\tilde{\rho_n}(\tilde{\theta}_1,\dots,\tilde{\theta}_n|A)_L + O(\mathrm{e}^{-\mu L}) \tag{63}$$

where the summation runs over all subsets A of $\{1,2,\dots n\}$. For any such subset, we define the appropriate sub-determinant

$$\tilde{\rho}_n(\tilde{\theta}_1,\dots,\tilde{\theta}_n|A) = \det \mathcal{J}_A(\tilde{\theta}_1,\dots,\tilde{\theta}_n) \tag{64}$$

of the $n\times n$ Bethe-Yang Jacobi matrix

$$\mathcal{J}(\tilde{\theta}_1,\dots,\tilde{\theta}_n)_{kl} = \frac{\partial Q_k(\theta_1,\dots,\theta_n)}{\partial\theta_l} \tag{65}$$

where $\mathcal{J}_A$ is obtained by deleting the rows and columns corresponding to the subset of indices A. The determinant of the empty sub-matrix (i.e. when $A=\{1,2,\dots n\}$) is defined to equal 1 by convention. Note also that diagonal matrix elements have no space-time dependence at all, therefore (63) is true both for operators located on the defect and in the bulk.

We remark for bulk theories on a spatial circle without defects, there exists another class of matrix elements with disconnected contributions when there is a particle of exactly zero momentum in both states. However, due to the presence of the defect this class is absent here. For example, from (55) it follows that the existence of a state with a single stationary particle would require

$$T_-(\theta=0)=1$$

but this is not satisfied for any finite value of the defect parameter b. The only class of matrix elements that has disconnected pieces at more than isolated values of L is the diagonal one treated above.

4 CFT

In order to explain the main building blocks of both the defect scaling LY model UV description and the TCSA method, I will summarize some facts about conformal field theories (CFT). This section will be mainly based on [10] and [14].

4.1 Conformal algebra

In any spacetime dimensions the Poincaré group can be extended with spacetime transformations, which do not preserve the metric, but they change it with (maybe space dependent) scalar factor

[11] the $(-1)^{|A|}$ therm is numerically well proved, and will be explained in [2].

$$g'(x') = \Omega(x)g(x) \tag{66}$$

This can be understand as the generalization of scale transformation (where Ω would be a constant).

Usually for RFTs scale invariance implies conformal invariance. In 2D this is proved [21], and in higher dimension counterexamples are rare (for a counterexample see [12]). Concrete examples of CFTs are the Maxwell's equations, in general zero mass free field theories or the N=4 SUSY Yang Mills in 4 dimension.

It can be shown, that in this case the symmetry group is of course bigger, than in the Poincaré case. However if the dimension (space+time) is greater then 2 it is still a finite dimensional Lie group, with two special Lie algebra generators, the D-dilatation and the so called special conformal transformation K^μ.

The commutators of the algebra can be calculated and its name is the conformal algebra.

$$[D, P_\mu] = iP_\mu \tag{67}$$
$$[D, K_\mu] = -iK_\mu \tag{68}$$
$$[K_\mu, P_\nu] = 2i(\eta_{\mu\nu}D - L_{\mu\nu}) \tag{69}$$
$$[K_\rho, L_{\mu\nu}] = i(\eta_{\rho\mu}K_\nu - \eta_{\rho\nu}K_\mu) \tag{70}$$
$$[P_\rho, L_{\mu\nu}] = i(\eta_{\rho\mu}P_\nu - \eta_{\rho\nu}P_\mu) \tag{71}$$
$$[L_{\mu\nu}, L_{\rho\sigma}] = i(\eta_{\nu\rho}L_{\mu\sigma} + \eta_{\mu\sigma}L_{\nu\rho} - \eta_{\mu\rho}L_{\nu\sigma} - \eta_{\nu\sigma}L_{\mu\rho}) \tag{72}$$

If we are dealing with field theory, this algebra should be represented on the fields. We can choose fields to transform under dilatation as:

$$\phi'(x') = \left|\frac{\partial x'}{\partial x}\right|^{-\Delta/d} \phi(x) \tag{73}$$

and label them by their Δ the so called conformal weight. These fields are called quasi-primary.

4.2 Witt algebra

In two dimension, there is an interesting situation. The conformal group is still finite dimensional, but we can extend the algebra by elements, which do not represent a globally invertible transformation, nevertheless if we choose any finite domain in the space, we can choose a small enough transformation generated by this extra generators to get a well defined (bijective) map between the domain and its image. These are the so called local conformal transformations, and in 2D its better to talk on the language of complex numbers and functions.

Lets deal first with an Euclidean theory in 2D, and let be the coordinates x, y. Now we can introduce new complex coordinates:

$$z = x + iy \tag{74}$$
$$\bar{z} = x - iy \tag{75}$$

Of course we would need just one of these (for example z) to completely determine a point if x and y are real, but in some cases we would like to analytically continuate the coordinates in which case z and $\bar{z}$ will be not complex conjugate pairs.

In this notation we can represent coordinate transformations as complex functions mappings from the complex plain (or more generally from the Riemann sphere) to itself.

$$z' = w(z) = w^0(x, y) + iw^1(x, y) \tag{76}$$

If we write down what conformal invariance means on this language, we discover, that this is nothing else, but the Cauchy–Riemann, or anti Cauchy–Riemann equations for the mapping.

$$\frac{\partial w^1}{\partial x} = \frac{\partial w^0}{\partial y} \quad \text{and} \quad \frac{\partial w^0}{\partial x} = -\frac{\partial w^1}{\partial y} \tag{77}$$

Or

$$\frac{\partial w^1}{\partial x} = -\frac{\partial w^0}{\partial y} \quad \text{and} \quad \frac{\partial w^0}{\partial x} = \frac{\partial w^1}{\partial y} \tag{78}$$

We can shorten the notation, if we take the definition of z and $\bar{z}$ as a change of variables. We introduce partial derivatives respect to them:

$$\partial_z = \frac{1}{2}(\partial_x - i\partial_y) \tag{79}$$

$$\partial_{\bar{z}} = \frac{1}{2}(\partial_x + i\partial_y) \tag{80}$$

In this notation the (77) and (78) are the following:

$$\partial_{\bar{z}} w(z, \bar{z}) = 0 \tag{81}$$

$$\partial_z w(z, \bar{z}) = 0 \tag{82}$$

(This notation gives back the standard derivation defined by limits in the analytic case, but can be used to derive non analytic functions as well.)

Now we want to deal just with infinetisimal transformations, which are close to the identity map. Due to the identity map is holomorphic, we will deal just with the holomorphic part.

Normally if we determine a complex mapping $w(z)$ of z then we also determined the function $\bar{w}(\bar{z})$ which maps $\bar{z} \to \bar{z}'$. However in this point we want to split these two functions, and let them to be independent.

The reality condition for x and y can be recovered, if we use the constraint: $\bar{w}(\bar{z}) = w(\bar{z}^*)^*$. (This will be also defined on the language of the algebra.)

Any local conformal transformation can be expressed as follows:

$$z' = z + \epsilon(z) \qquad \epsilon(z) = \sum_{n=-\infty}^{\infty} c_n z^{n+1} \tag{83}$$

$$\bar{z}' = \bar{z} + \bar{\epsilon}(\bar{z}) \qquad \bar{\epsilon}(\bar{z}) = \sum_{n=-\infty}^{\infty} \bar{c}_n \bar{z}^{n+1} \tag{84}$$

If we have a function $\phi(z, \bar{z})$, then it will infinitesimally change as:

$$\delta\phi(z, \bar{z}) = \sum_{n=-\infty}^{\infty} c_n \ell_n \phi(z, \bar{z}) + \bar{c}_n \bar{\ell}_n \phi(z, \bar{z}) \tag{85}$$

Where the differencial operators ℓ_n and $\bar{\ell}_n$ are defined as:

$$\ell_n = -z^{n+1}\partial_z \tag{86}$$

$$\bar{\ell}_n = -\bar{z}^{n+1}\partial_{\bar{z}} \tag{87}$$

We can compute their commutators and get the infinite dimensional Witt algebra:

$$[\ell_n, \ell_m] = (n-m)\ell_{n+m} \tag{88}$$

$$[\bar{\ell}_n, \bar{\ell}_m] = (n-m)\bar{\ell}_{n+m} \tag{89}$$

$$[\ell_n, \bar{\ell}_m] = 0 \tag{90}$$

The equation (90) explains, why is natural to split functions on z and $\bar{z}$. The reality condition of x and y here would force, to build up the algebra as a real vector space, spanned by $\ell_n + \bar{\ell}_n$ and $i(\ell_n - \bar{\ell}_n)$.

This algebra contains $\{\ell_{-1}, \ell_0, \ell_1, \bar{\ell}_{-1}, \bar{\ell}_0, \bar{\ell}_1\}$ as subalgebra, which represents the global conformal transformations.

$\ell_{-1} + \bar{\ell}_{-1}$ and $i(\ell_{-1} - \bar{\ell}_{-1})$ the space shifts, $\ell_0 + \bar{\ell}_0$ the dilatation, $i(\ell_0 - \bar{\ell}_0)$ the rotation, $\ell_1 + \bar{\ell}_1$ and $i(\ell_1 - \bar{\ell}_1)$ the special conformal transformations.

This complex formalism can be unfamiliar for the first sight, but basically we do the same when we calculate electrostatic problems in 2D and we use conformal maps.

4.3 Exponentional mapping

In every derivation in 4.5 we assumed that the space is flat, and so globally $\mathbb{R}^d$, however we want to investigate theories confined into a finite volume. To bypass this problem, in CFTs we can use exponentional mappings [10].

Let be the theory defined on a spacetime cylinder with periodic boundary condition: $\phi(0, t) = \phi(L, t)$. We can introduce two complex parameters:

$$\zeta = t + ix \tag{91}$$

$$\bar{\zeta} = t - ix \tag{92}$$

By reason of we want to deal with conformal invariant theories, or a perturbed one, with fields which transforms simple under conformal maps, we can use the exponential function to map the cylinder to the complex plane:

$$z = e^{\frac{2\pi}{L}\zeta} \tag{93}$$

$$\bar{z} = e^{\frac{2\pi}{L}\bar{\zeta}} \tag{94}$$

The visualization of this map can be seen on figure 7.

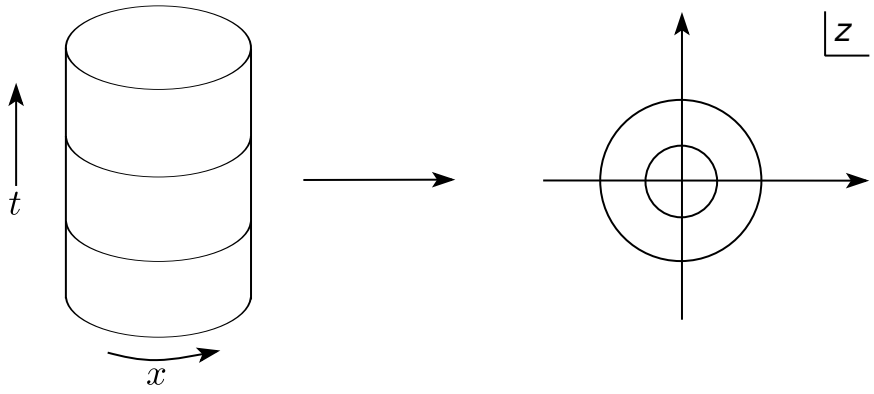

Figure 7: Exponentional mapping

The exponentional map maps the infinite past points into one point on the cylinder, namely into 0, and the infinite future points to the ∞. Equal time points will appear as concentric circles, and a time shift on the cylinder will be equal of the dilatation on the plane.

While the local conformal transformations were written in terms of Laurent series, every single generator defined in (86) and (87) behaves nicely on a ring, which do not contains 0 or ∞. It means, that these transformations are well defined on every finite time interval on the cylinder.

4.4 Radial ordering and OPE

In the operator formalism of QFT we use time ordered products, to make these expressions definite. On the plane radial ordering $\mathcal{R}$ plays the same role. Explicitly (for bosonic fields):

$$\mathcal{R}\phi(z)\psi(w) = \begin{cases} \phi(z)\psi(w) & |z| > |w| \\ \psi(w)\phi(z) & |z| < |w| \end{cases} \tag{95}$$

In the following sections we use every time radial ordered products implicitly.

If we are dealing with a QFT, we would expect that due to quantum fluctuations $\langle\phi(z)\phi(w)\rangle$ diverge if $w \to z$. Generally we can express products of local fields as:

$$\phi_i(z)\phi_j(w) = \sum_k C_{ij}^k(z-w)\phi_k(w) \tag{96}$$

where the $C_{ij}^k(x)$ function can be singular when $x \to 0$. This is the operator product expansion (OPE).

In CFTs the divergent terms are power like, and the exponents are well determined for primary fields and their descendants (which will be introduced in subsection 4.6).

By using powerful complex analysis, these expansions are useful to calculate commutators of operators, which are space integrals of local fields: (Space integral on the cylinder corresponds to contour integral on the plane). For example if

$$A = \oint a(z)\mathrm{d}z, \tag{97}$$

and

$$B = \oint b(z)\mathrm{d}z, \tag{98}$$

then

$$[A, B] = \oint_0 \mathrm{d}w \oint_w \mathrm{d}z a(z)b(w). \tag{99}$$

If we now how to expand $a(z)b(w)$ to Laurent series, we can calculate the integrals by the residue theorem.

4.5 The Virasoro algebra

Now we want to calculate, what are the quantum generators of local conformal transformations, and what is their algebra.

In a QFT there is always possible to construct an energy momentum tensor which generates all types of coordinate transformations (and not just space and time shifts). Because of the conformal symmetry, we assume, that this is trace less. Then if we apply the complex variable change to z and $\bar{z}$, we will see that only $T_{zz}(z)$ and $T_{\bar{z}\bar{z}}(\bar{z})$ will be nonvanishing. To shorten formulas, we define them as $T(z)$ and $T(\bar{z})$.

To go further we need the OPE of the energy momentum tensor with itself. It can be straightforwardly calculated for simple models like the free boson or fermion. We can use conformal invariance to find out what can be the general form, and finally every concrete example can be generalized into the form:

$$T(z)T(w) = \frac{c/2}{(z-w)^4} + \frac{2T(w)}{(z-w)^2} + \frac{\partial T}{(z-w)} + \dots \tag{100}$$

Where c is the central charge of the theory (for example for free boson $c = 1$). [12]

This central charge have also some nice properties, for example for non interacting fields in the theory it is additive. It breaks just "softly" the conformal invariance, because it has no effect on the global conformal group action. Furthermore this central charge is responsible for the finite size (or curvature) effects in the theory.

Using this energy momentum tensor we can construct a generator of local conformal transformation $\epsilon(z)$

$$Q_\epsilon = \frac{1}{2\pi i} \oint \mathrm{d}z \epsilon(z) T(z) \tag{101}$$

We can expand $T(z)$ to Laurent series:

[12] In general c and $\bar{c}$ for antiholomorphic energy momentum tensor could be independent, but if the theory on the cylinder is Lorentz invariant, and the $\langle T_{\mu\nu}(p)T_{\rho\sigma}(-p)\rangle$ is conserved, then $c = \bar{c}$.

$$T(z) = \sum_{k\in\mathbb{Z}} z^{-n-2} L_n, \tag{102}$$

$$L_n = \frac{1}{2\pi i} \oint \mathrm{d}z z^{n+1} T(z). \tag{103}$$

From (99) and (100) we can get the algebra of this operators, called the Virasoro algebra:

$$[L_n, L_m] = (n-m)L_{n+m} + \frac{c}{12} n(n^2-1)\delta_{n+m,0} \tag{104}$$

4.6 Primary Fields

In 2D conformal field theory we call a field primary, if it transforms under local conformal transformation as:

$$\phi'(w,\bar{w}) = \left(\frac{\mathrm{d}w}{\mathrm{d}z}\right)^{-h} \left(\frac{\mathrm{d}\bar{w}}{\mathrm{d}\bar{z}}\right)^{-\bar{h}} \phi(z,\bar{z}) \tag{105}$$

We call h and $\bar{h}$ the holomorphic and antiholomorphic conformal dimension (or left and right weight) of the field. From these the previously introduced scaling dimension and spin can be recovered as the sum and the difference:

$$\Delta = h + \bar{h} \qquad s = h - \bar{h} \tag{106}$$

On the language of Virasoro generators this transformation property means, that:

$$[L_n, \phi(w,\bar{w})] = h(n+1)w^n \phi(w,\bar{w}) + w^{n+1}\partial\phi(w,\bar{w}) \tag{107}$$

This property is more restrictive then to be a quasi primary field, because there we prescribed their transformation just under the global conformal transformations. An example of a quasi primary field, which is not primary is the energy momentum tensor.

Fields, which are not primary, are called in general secondary. For example if $h \neq 0$ then its derivatives are secondary.

The asymptotic OPE for primary fields is very simple [14]:

$$\phi_i(z,\bar{z})\phi_j(w,\bar{w}) \sim \sum_k C_{ij}^k (z-w)^{h_k - h_i - h_j} (\bar{z}-\bar{w})^{\bar{h}_k - \bar{h}_i - \bar{h}_j} \phi_k(w,\bar{w}) \tag{108}$$

Where C_{ij}^k are the so called structural constants.

Basically if we can determine all C_{ij}^k it results the full description of the theory.

4.7 State Operator identification

If we are dealing with a QFT we have to set the vacuum state of the theory $|0\rangle$.

We prescribe for this state, to be invariant under global conformal transformations on the plane. It sets the vacuum energy to 0. We prescribe also, that $T(z)|0\rangle$ and $T(\bar{z})|0\rangle$ are well defined in the origin.

These prescriptions imply that

$$L_n|0\rangle = 0 \quad \bar{L}_n|0\rangle = 0 \quad n \geq -1 \tag{109}$$

We note, that this definition of the vacuum state, is not always the lowest energy level. Especially in non unitary theories, like the LY model it can happen, that a lower energy state is present, however this is not invariant under the global conformal algebra.

For every primary field with conformal weights $(h, \bar{h})$, we can define a state as follows:

$$|h, \bar{h}\rangle = \lim_{z,\bar{z}\to 0} \phi(z, \bar{z})\,|0\rangle, \tag{110}$$

and its adjoint as:

$$\langle h, \bar{h}| = \lim_{z,\bar{z}\to 0} \langle 0|\bar{z}^{-2h} z^{-2\bar{h}} \phi(1/\bar{z}, 1/z). \tag{111}$$

This definition of the adjoint is nontrivial, and is adopted, to have well defined scalar product.

Applying (107) we conclude, that:

$$L_0|h, \bar{h}\rangle = h|h, \bar{h}\rangle \quad \bar{L}_0|h, \bar{h}\rangle = \bar{h}|h, \bar{h}\rangle \tag{112}$$

and

$$L_n|h, \bar{h}\rangle = 0 \quad \bar{L}_n|h, \bar{h}\rangle = 0 \quad n \geq 0 \tag{113}$$

While from the Virasoro algebra:

$$[L_0, L_{-m}] = mL_{-m} \quad [\bar{L}_0, \bar{L}_{-m}] = m\bar{L}_{-m} \tag{114}$$

These L_n operators can be viewed as annihilation operators if $n > 0$ and creation operators if $n < 0$. Now to shorten notation we deal just with the holomorphic part.

From these we can build up the descendant states of $|h\rangle$ as:

$$L_{-k_1} L_{-k_2} \dots L_{-k_n}|h\rangle \ ^{13} \tag{115}$$

This state is at level $N = k_1 + k_2 + \dots + k_n$, and it has conformal weight:

$$L_0 \ L_{-k_1} L_{-k_2} \dots L_{-k_n}|h\rangle = (N + h) L_{-k_1} L_{-k_2} \dots L_{-k_n}|h\rangle \tag{116}$$

We call all descendant states of a highest weight state $|h\rangle$ Verma module, which is an irreducible representation of the Virasoro algebra [14]:

$$\mathcal{V}_h = Span\{L_{-k_1} L_{-k_2} \dots L_{-k_n}|h\rangle \ | n \in \mathbb{N}, k_1, k_2, \dots k_n \in \mathbb{N}\} \tag{117}$$

If we take to account the holomorphic part also, then we can write down the full vector space of descendant states:

$$\mathcal{V}_{h\bar{h}} = \mathcal{V}_h \otimes \bar{\mathcal{V}}_{\bar{h}} \tag{118}$$

If we can identify all highest weight states in the theory, then we can build up the Hilbert space from these Verma modules:

$$\mathcal{H} = \mathcal{V}_1 \oplus \mathcal{V}_2 \oplus \dots \tag{119}$$

[13] These descendant states are connected with derivatives of the fields.

[14] the effect of zero normed states, and linearly not independent levels will be discussed in section 5

4.8 Minimal models

After getting familiar with calculating quantities in CFTs motivated by some simple physical systems, we can start to deal with abstract CFTs, which are defined just by their conformal charge, and a set of primary fields defined by its conformal weights.

It turns out, that if we start with finite number of primary fields, and we choose the central charge and the weights of the primary fields carefully, then we can get fully solvable CFTs, the so called minimal models.

In this point there is a question, if this kind of theories really describe anything? The question is natural, because non of the simple examples like the free boson has finite number of primary fields.

However the answer is yes, and we can find a variety of statistical and solid state physical models for example Ising or 3 state Potts model [10] which can be described by a minimal model in the continuum limit.

In minimal models the Verma modules are "smaller", what means, that on some levels linearly dependent states can occur.

It is shown in [10], that these minimal models can be parametrized by two $p, q > 2$ relative prime numbers, in which case the central charge in $\mathcal{M}_{p,q}$ reads as:

$$c = 1 - 6\frac{(p-q)^2}{pq} \tag{120}$$

And we can choose primary fields in the theory, labeled by two natural numbers r, s, where $r \in \{1, 2, \dots p-1\}$, and $s \in \{1, 2, \dots q-1\}$. Its conformal weight will be:

$$h_{r,s} = \frac{(ps - qr)^2 - (p-q)^2}{4pq} \tag{121}$$

Not all minimal models are unitary. It can be shoved [10] that the unitarity condition is $c > 0$, $h > 0$. The simplest non trivial minimal model $\mathcal{M}_{2,5}$ is non unitary as well.

It has central charge $c = -22/5$, and the only nontrivial conformal weight can be $h = -1/5$. Nevertheless the model is non unitary, it can be identified with the conformal LY model, which mathematically describes 2D Ising model in imaginary magnetic field.

5 TCSA

As we saw in subsection 2.2 we can define a theory not just in infinite but also in finite volume. In this case we have to specify the boundary conditions.

When the size of the box with some boundary conditions is much bigger than the DeBroglie wavelength of the particles inside, then the S-matrix and other scattering matrices like the transmission matrix at the defect are well defined.

We can try to choose a numerical method, to calculate some quantities of the theory (typically energy levels, and form factors of some operators). However we will discover, that mainly every quantity in the theory has some finite size effect.

Traditionally we try to avoid them, and get results for infinite volumes, by increasing the volume or by finite size extrapolations. However there is a method, where these finite size effect can help us to understand better the theory [27].

We can recognize, that when we define the theory in very small (according the rest mass of the particles) volumes, then we get asymptotically a conformal field theory. This is because the quantization condition for the particles momentum requires to be very big, and we end up at an extremely relativistic situation, where the rest mass of particles can be neglected.

If we could identify the conformal limit of a theory, then we could exactly solve it in small volumes, and then try to add perturbation to it in the language of CFT. If we can choose a good perturbation, which vanishes in the conformal limit, and rises as some positive power of volume (so the perturbation is relevant) then we can use the truncated conformal space approach to numerically check if we get back the asked theory, and also to measure quantities in the model. [15]

This method was first invited and used by Zamolodchikov and Yurov to check the connection between LY and scaling LY model [28].

In truncated conformal space approach (TCSA) we build up the Hilbert space of a CFT for a finite number of states (we cut the Hilbert space on some energy level), then we calculate the matrix elements of the chosen perturbing operators, and we diagonalize this matrix at different volumes to get energies, and eigenvectors of the Hamiltonian.

It is variational and not a perturbative method, that is why it does not suffer of problems of standard perturbative methods. Of course it has also errors because of the truncation of the Hilbert space, but theoretically it can achieve any predefined precision by rising the cut if $h, \bar{h} < 1/2$ for every highest weight state. If there are states with $h \geq 1/2$, an appropriate renormalization method can be used, what is not considered in this work.

The presented quick overview here will be based on [27].

5.1 The truncated Hilbert space

First we have to build up a finite dimensional vector space which contains every energy eigenstate below some predefined energy E_{cut}. The Hamilton operator on the plane can be expressed by the dilatation operator:

$$H = \frac{2\pi}{L}\left(L_0 + \bar{L}_0 - \frac{c}{12}\right) \tag{122}$$

If we would know the whole Hilbert space of the theory, then the definition would read as:

$$\mathcal{H}_{cut} = Span\left\{|\psi\rangle \in \mathcal{H} : H_0|\psi\rangle = E|\psi\rangle, E \leq E_{cut}\right\} \tag{123}$$

To avoid the volume dependence of the truncated Hilbert space, we introduce a dimensionless variable:

$$cut = \frac{E_{cut}L}{2\pi} \tag{124}$$

which practically determine the highest level in Verma modules. According to eq. (116):

$$\left(L_0 + \bar{L}_0\right)|\psi\rangle = (N + \bar{N} + h + \bar{h})|\psi\rangle \tag{125}$$

$$N + \bar{N} + h + \bar{h} - \frac{c}{12} \leq cut \tag{126}$$

[15] Irrelevant and marginal perturbations are sometimes useful also.

Due to that, the main task is to build up Verma modules up to some predefined level N. To take into account the linearly dependent vectors in minimal models, we have to set the Virasoro inner product of descendant states.

$$\langle h,\bar{h}|\bar{L}_{\ell'_{m'}}\dots L_{k'_{n'}}\dots L_{-k_1}\dots\bar{L}_{-\ell_1}\dots|h,\bar{h}\rangle^{16} \tag{127}$$

We can use the Virasoro algebra to change the order of $+$ and $-$ index terms. Because of that only the L_0 operators will give non zero elements, and finally the scalar product will be:

$$C\langle h,\bar{h}|h,\bar{h}\rangle\ ;\quad C\in\mathbb{R}$$

If we set the scalar product of highest weight states, then every Virasoro inner product of descendant states can be calculated. (Furthermore it can be implemented for example in `Mathematica` .)

Now I show a recursive method, to determine a Verma module up to level N, where the vectors are naturally labeled by their level [27].

Building up the Hilbert space: We want to build up a basis of Verman module up to level N, by taking to account, that not every strings of the form $L_{-k_1}\dots L_{-k_n}|h,\bar{h}\rangle$ are linearly independent. We define Bas_n recursively:

$$Bas_0=|h,\bar{h}\rangle \tag{128}$$

$$\widetilde{Bas}_n=L_{-n}Bas_0\bigcup L_{-(n-1)}Bas_1\bigcup\dots\bigcup L_{-1}Bas_{n-1} \tag{129}$$

Then we build up Bas_n from $\widetilde{Bas}_n$. We find the first non zero norm in $\widetilde{Bas}_n$ and we put to Bas_n. If we have already k vectors in Bas_n, then we try to find a new one from $\widetilde{Bas}_n$, to have a nonsingular $(k+1)\times(k+1)$ matrix from Virasoro inner products. If we can find such a vector, then we put it to Bas_n, and if we tried all from $\widetilde{Bas}_n$, then we end the process.

This basis will be not orthogonal, but we can calculate its Gramm matrix:

$$G_{ij}=\langle i|j\rangle \tag{130}$$

In some cases the Hilbert space is explicitly known. Fortunately for the $\mathcal{M}_{2,5}$ conformal LY model it can be explicitly written as:

$$L_{-n_1}\dots L_{-n_m}|0\rangle\ ;\qquad n_m\geq 2\ ;\qquad n_i\geq n_{i+1}+2 \tag{131}$$

$$L_{-n_1}\dots L_{-n_m}|h\rangle\ ;\qquad n_m\geq 1\ ;\qquad n_i\geq n_{i+1}+2 \tag{132}$$

$$\sum_{i=1}^{m}n_i\leq N \tag{133}$$

And inner products have to be set as:

$$\langle 0|0\rangle=1 \tag{134}$$

[16] $L_k^\dagger=L_{-k}$ [10].

$$\langle h,h|h,h\rangle = -1 \ ^{17} \tag{135}$$

5.2 Hamiltonian action matrix

We can add perturbation(s) to the CFT Hamiltonian expressed by the primary fields. Usually these are space integrals of the fields, which can be mapped to the plane. In order to determine matrix elements of primary fields, we have to know the structural constants of the theory. If we know them, then we can determine the perturbed Hamiltonian matrix elements:

$$\langle i|H^{pert}|j\rangle$$

However we need the action matrix of operator $H : \mathcal{H}_{cut} \to \mathcal{H}_{cut}$

$$H = H_0 + H^{pert} \tag{136}$$

$$H^{pert}|i\rangle = \sum_k H^{pert}_{ki}|k\rangle. \tag{137}$$

$$\langle j|H^{pert}|i\rangle = \sum_k H^{pert}_{ki} G_{jk}, \tag{138}$$

$$H^{pert}_{ki} = \sum_j \left(G^{-1}\right)_{kj} \langle j|H^{pert}|i\rangle \tag{139}$$

In order to make the Hamiltonian suitable for numerical calculation, we divide it with a characteristic energy scale of the theory. If perturbations results a massive theory dividing by the mass is the simplest solution.

6 The defect scaling LY model

6.1 The scaling LY model

It was shown by Zamolodchikov [30], that the scaling LY model can be viewed, as the perturbation of the simplest nontrivial minimal model $\mathcal{M}_{2,5}$ with its unique nontrivial relevant perturbation $\phi_{1,2}$. The central charge, and the scaling dimension are: $c = -22/5$ and $h = -1/5$. The primary field $\Phi = \phi_{1,2}$ is spin less, it has both conformal weights $h = \bar{h} = -1/5$.

The Hilbert space is build on $|0\rangle$ and $|h,h\rangle$:

$$\mathcal{H} = \mathcal{V}_0 \otimes \bar{\mathcal{V}}_0 + \mathcal{V}_{-1/5} \otimes \bar{\mathcal{V}}_{-1/5} \tag{140}$$

Formally the action of the scaling LY model reads:

$$S = S_0 + \lambda \int \mathrm{d}y \int \mathrm{d}x \Phi(x,y) \tag{141}$$

Where S_0 is the pure conformal action.

[17] The negative inner product is a consequence of non unitarity.

The relation between the mass gap of the theory, and the coupling constant was determined:

$$m = \kappa \lambda^{\frac{5}{12}} \quad ; \qquad \kappa = \frac{2^{\frac{19}{12}}\sqrt{\pi}}{5^{\frac{5}{16}}} \frac{\left(\Gamma\left(\frac{3}{5}\right)\Gamma\left(\frac{4}{5}\right)\right)^{\frac{5}{12}}}{\Gamma\left(\frac{2}{3}\right)\Gamma\left(\frac{5}{6}\right)} \approx 2.642944. \tag{142}$$

To deal with finite size effects, and to be able to use TCSA, we define the theory on a cylinder with length L:

$$S = S_0 + \lambda \int \mathrm{d}y \int_L \mathrm{d}x \Phi(x, y) \tag{143}$$

We can rewrite this definition to Hamiltonian formalism, and map the cylinder to the complex plane by the exponentional map. As result, we get the Hamiltonian on the plane:

$$H = \frac{2\pi}{L}\left(L_0 + \bar{L}_0 - \frac{c}{12} - \lambda\left(\frac{L}{2\pi}\right)^{2-2h} \int_0^{2\pi} d\theta\, \Phi\left(\mathrm{e}^{i\theta}, \mathrm{e}^{-i\theta}\right)\right) \tag{144}$$

Here we can immediately check, that the perturbation is relevant, because it rises with positive power of the volume: $L^{7/5}$. In the defectless theory, due to rotation invariance the angle integral can be expressed by $\Phi(1,1)$. However in case of the defect we have to evaluate it correctly, and that is why was kept this general form.

We can make the expression dimensionless, by deviding with m

$$\frac{H}{m} = \frac{2\pi}{mL}\left(L_0 + \bar{L}_0 - \frac{c}{12} - \left(\frac{mL}{2\pi\kappa}\right)^{2-2h} \int_0^{2\pi} d\theta\, \Phi\left(\mathrm{e}^{i\theta}, \mathrm{e}^{-i\theta}\right)\right) \tag{145}$$

To determine the matrix elements of $\phi(1,1)$ we need:

$$\langle h, h|\phi(1,1)|h, h\rangle = -\alpha^2\beta \tag{146}$$

$$\alpha = \sqrt{\frac{\Gamma\left(\frac{1}{5}\right)\Gamma\left(\frac{6}{5}\right)}{\Gamma\left(\frac{3}{5}\right)\Gamma\left(\frac{4}{5}\right)}}\,, \qquad \beta = \sqrt{\frac{2}{1+\sqrt{5}}}. \tag{147}$$

From these ingredients the Hamiltonian action matrix for TCSA can be build.

6.2 Definition of defect scaling LY model

Now we want to define the scaling LY model with a defect line as the perturbation of a CFT. We can use the same $\mathcal{M}_{2,5}$ minimal model, but the presence of the defect line will change the Hilbert space, and the operator content of the theory.

Let first see the result of the exponentional mapping of a cylinder with one defect line:

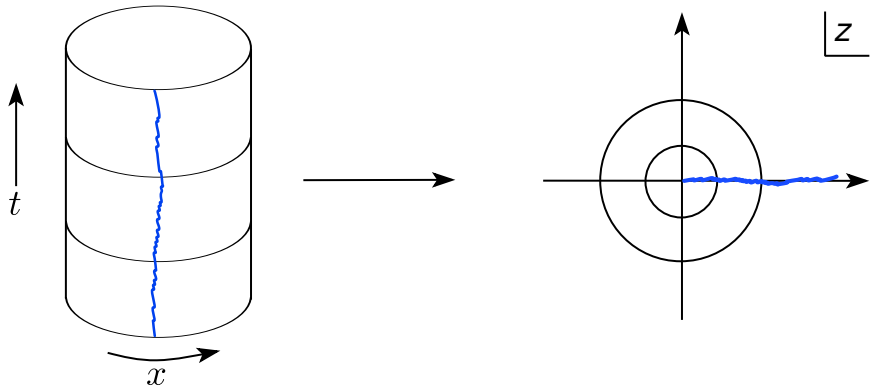

Figure 8: Exponentional mapping of the defect theory

While the defect is topological, it means that the whole stress energy tensor is insensitive for the defect. It implies, that the defect fortunately do not modify the symmetry algebra of the system (unlike boundary).

However if we apply an exponential map from a cylinder to the plane, we can see that the defect runs on the whole half line of the plane. It implies, that there are 3 special kind of places on the plane, which cannot be transformed by conformal transformation to each other.

There are points which has finite neighborhood without defect line, there are points on the line, and the origin is also special, because it is on the endpoint of the defect line.

This expectation ruins the state operator identification, but with the help of modular invariance (where the main idea is that in euclidean theory space and "time" can be freely interchanged) one can build up a Hilbert space from the basic (boundary less) CFT and introduce possible primary fields, both defined on the boundary and on the bulk [20]. This set up and its numerical check was done in [15].

Due to the nontrivial defect, the Hilbert space of the defect Lee-Yang model

$$\mathcal{H} = \mathcal{V}_0 \otimes \bar{\mathcal{V}}_{-\frac{1}{5}} + \mathcal{V}_{-\frac{1}{5}} \otimes \bar{\mathcal{V}}_0 + \mathcal{V}_{-\frac{1}{5}} \otimes \bar{\mathcal{V}}_{-\frac{1}{5}} \tag{148}$$

does not coincide with the operator space localized on the defect which is

$$\mathcal{V}_0 \otimes \bar{\mathcal{V}}_0 + \mathcal{V}_{-\frac{1}{5}} \otimes \bar{\mathcal{V}}_0 + \mathcal{V}_0 \otimes \bar{\mathcal{V}}_{-\frac{1}{5}} + 2\mathcal{V}_{-\frac{1}{5}} \otimes \bar{\mathcal{V}}_{-\frac{1}{5}} = [\mathbb{I}] + [\varphi] + [\bar{\varphi}] + [\Phi_{\pm}] \tag{149}$$

The action of the defect scaling LY model defined on the cylinder reads as:

$$S = S_0 + \lambda \int \mathrm{d}y \int \mathrm{d}x \, \Phi(x, y) + \mu \int \mathrm{d}y \, \varphi(y) + \bar{\mu} \int \mathrm{d}y \, \bar{\varphi}(y) \,, \tag{150}$$

It can be mapped to the plane, where the Hamiltonian has the form:

$$H = \frac{2\pi}{L} \left(L_0 + \bar{L}_0 - \frac{c}{12} - \lambda \left(\frac{L}{2\pi} \right)^{\frac{12}{5}} \int_0^{2\pi} d\theta \, \Phi\left(\mathrm{e}^{i\theta}, \mathrm{e}^{-i\theta} \right) - \left(\frac{L}{2\pi} \right)^{\frac{6}{5}} (\mu\varphi(1) + \bar{\mu}\bar{\varphi}(1)) \right) \tag{151}$$

An appropriate momentum operator was found by conformal perturbation theory [5]:

$$P = \frac{2\pi}{L}\left(L_0 - \bar{L}_0 - \left(\frac{L}{2\pi}\right)^{\frac{6}{5}}\mu\varphi(1) + \left(\frac{L}{2\pi}\right)^{\frac{6}{5}}\bar{\mu}\bar{\varphi}(1)\right) \tag{152}$$

Integrability dictates

$$[H, P] = 0. \tag{153}$$

It can be satisfied, if we require the following relation between the coupling constants:

$$\mu\bar{\mu} = -i\lambda\frac{1}{2\tilde{c}} = \xi_1^2\lambda \tag{154}$$

where

$$\xi_1 = \sqrt{\frac{-i}{2\tilde{c}}} \approx 1.09989\,. \tag{155}$$

The link between μ, $\bar{\mu}$ and the b defect parameter defined in subsection 2.2 was also determined:

$$\mu = \xi_1\sqrt{\lambda}\mathrm{e}^{\frac{i\pi}{5}(b+3)} = -\xi_1\sqrt{\lambda}\mathrm{e}^{\frac{i\pi}{5}(b-2)}, \tag{156}$$

$$\bar{\mu} = \xi_1\sqrt{\lambda}\mathrm{e}^{-\frac{i\pi}{5}(b+3)} = -\xi_1\sqrt{\lambda}\mathrm{e}^{-\frac{i\pi}{5}(b-2)}, \tag{157}$$

The relation between m and λ remains the same, as in the bulk theory.

To prepare the operators for numerical investigations, we divide them by m. Hamiltonian and momentum action matrices read:

$$\frac{H}{m} = \frac{2\pi}{mL}\left(L_0 + \bar{L}_0 + \frac{11}{30} + \xi\left(\frac{L}{2\pi\kappa}\right)^{1+\frac{1}{5}}\left(a(G^{-1}\hat{\varphi})_{jk} + \bar{a}(G^{-1}\hat{\bar{\varphi}})_{jk}\right) - \left(\frac{L}{2\pi\kappa}\right)^{2+\frac{2}{5}}(G^{-1}\hat{\Phi})_{jk}\right) \tag{158}$$

$$\frac{P}{m} = \frac{2\pi}{mL}\left(L_0 - \bar{L}_0 + \xi\left(\frac{L}{2\pi\kappa}\right)^{1+\frac{1}{5}}\left(a(G^{-1}\hat{\varphi})_{jk} - \bar{a}(G^{-1}\hat{\bar{\varphi}})_{jk}\right)\right) \tag{159}$$

where matrices with hat are the matrix elements: $\hat{\varphi}_{jk} = \langle j|\varphi(1)|k\rangle$, $\hat{\bar{\varphi}}_{jk} = \langle j|\bar{\varphi}(1)|k\rangle$, $\hat{\Phi}_{jk} = \langle j|\Phi(1,1)|k\rangle P_{jk}$ and the matrix

$$P_{jk} = \begin{cases} 2\pi & \text{if } h_k - \bar{h}_k - h_j + \bar{h}_j = 0 \\ 2e^{i\pi(h_k-\bar{h}_k-h_j+\bar{h}_j)}\frac{\sin\pi(h_k-\bar{h}_k-h_j+\bar{h}_j)}{(h_k-\bar{h}_k-h_j+\bar{h}_j)} & \text{otherwise} \end{cases} \tag{160}$$

Every other parameter written explicitly: $\xi = \sqrt[4]{\frac{5}{8} + \frac{3\sqrt{5}}{8}}$, $a = e^{i\frac{\pi}{5}(b-2)}$ and $\bar{a} = e^{-i\frac{\pi}{5}(b-2)}$.

The structural constants of the defect theory are already determined [15]. They can be found in appendix A and from these ingredients every matrix element can be calculated.

The numerical investigations of form factors based on these matrices is discussed in subsection 7.1.

6.3 Previously know form factors

The form factors of the left/right limits of the bulk operator $\Phi_{\mp}$ and the low lying form factors of the two chiral fields living only at the defects have been already calculated. The results are summarized in the following table [2]:

Operator	Q_1	Q_2
Φ_-	$\nu\sigma_1 + \bar{\nu}\bar{\sigma}_1 + \sqrt{3}$	$\sigma_1(v^2\sigma_2 + \sqrt{3}v\sigma_1 + \sigma_1\bar{\sigma}_1 + 1 + \sqrt{3}\bar{\nu}\bar{\sigma}_1 + \bar{\nu}^2\bar{\sigma}_2)$
Φ_+	$\nu\sigma_1 + \bar{\nu}\bar{\sigma}_1 - \sqrt{3}$	$\sigma_1(v^2\sigma_2 - \sqrt{3}v\sigma_1 + \sigma_1\bar{\sigma}_1 + 1 - \sqrt{3}\bar{\nu}\bar{\sigma}_1 + \bar{\nu}^2\bar{\sigma}_2)$
φ	$\bar{\sigma}_1$	$\sigma_1(\bar{\nu}\bar{\sigma}_2 + \nu)$
$\bar{\varphi}$	σ_1	$\sigma_1(\nu\sigma_2 + \bar{\nu})$

Table 1: The form factor solutions of the primary fields up to level 2

The exact vacuum expectation values also will be find in [2]:

$$\langle\varphi\rangle = i\frac{5}{12}\frac{\kappa^{\frac{6}{5}}}{\xi}e^{i\frac{\pi}{30}(12-b)} \qquad ; \qquad \langle\bar{\varphi}\rangle = -i\frac{5}{12}\frac{\kappa^{\frac{6}{5}}}{\xi}e^{-i\frac{\pi}{30}(12-b)} \tag{161}$$

My task was to find more form factor solutions for $\bar{\varphi}$, compatible with the recursion relations. This work and its numerical check can be read in section 7.

7 Results

7.1 Analytical results

In the end of subsection 2.3 recursion relations were derived for Q_n symmetrical Laurent polynomials, which are ingredients of the form factors. In subsection 6.3 the first 2 of them is presented. My task was to calculate higher order polynomials for operator $\bar{\varphi}$.

The recursion relations can be rewritten to the form:
Dynamical:

$$Q_n(u\omega, u\bar{\omega}, x_2, \dots x_{n-1}) = D_{n-1}(u, x_2, \dots, x_{n-1})Q_{n-1}(u, x_2, \dots, x_{n-1}) \tag{162}$$

$$D_{n-1}(u, x_2, \dots, x_{n-1}) = (\nu u + \bar{\nu}\bar{u})\, u \left(\prod_{i=2}^{n-1}(u + x_i)\right) \tag{163}$$

Kinematical:

$$Q_n(u, -u, x_2, \dots, x_{n-1}) = K_{n-2}(u, x_2, \dots, x_{n-1})Q_{n-2}(x_2, \dots, x_{n-1}) \tag{164}$$

$$\begin{aligned} K_{n-2}\left(u, x_2, \dots, x_{n-1}\right) \;=\; & (-1)^n \frac{u}{2\left(\omega - \bar{\omega}\right)}\left(u^2\nu^2 - 1 + \bar{u}^2\bar{\nu}^2\right) \\ & \left(\prod_{i=2}^{n-1}\left(\omega u + \bar{\omega}x_i\right)\left(\bar{\omega}u - \omega x_i\right) - \prod_{i=2}^{n-1}\left(\omega u - \bar{\omega}x_i\right)\left(\bar{\omega}u + \omega x_i\right)\right) \end{aligned} \tag{165}$$

And the first two polynomials are:

$$Q_1 = \sigma_1 \tag{166}$$
$$Q_2 = \bar{\nu}\sigma_1 + \nu\sigma_1\sigma_2 \tag{167}$$

In general we have to find Laurent polynomials, which are called Laurent, because $\bar{\sigma}_k(x_1, \ldots, x_n) = \sigma_k(x_1^{-1}, \ldots, x_n^{-1})$ can appear. (And they really appear in the form factors for φ.) However these $\bar{\sigma}_k$s can be expressed as $\bar{\sigma}_k = \sigma_{n-k}/\sigma_n$. Due to that a general Laurent polynomial can be expressed as:

$$Q_n = \sum_{\alpha_1,\ldots\alpha_{n-1}\in\mathbb{N},\alpha_n\in\mathbb{Z}} C_{\alpha_1,\ldots,\alpha_n}\sigma_1^{\alpha_1}\ldots\sigma_n^{\alpha_n} \tag{168}$$

These recursion relations do not determine uniquely the next coming Q_n polynomials. We can easily construct kernel polynomials of the kinematical and dynamical recursion relations, which give 0 if we apply the variable replacements.

$$\mathcal{K}_n^K = \prod_{i\leq j}(x_i + x_j) \tag{169}$$

$$\mathcal{K}_n^D = \prod_{i\leq j}((x_i + x_j)^2 - x_i x_j) \tag{170}$$

It means, that if we found a Laurent polynomial satisfying (162)(164), then every other which has the form:

$$Q'_n = Q_n + \mathcal{K}_n^D\mathcal{K}_n^K\left(\sum_{\alpha_1,\ldots\alpha_{n-1}\in\mathbb{N},\alpha_n\in\mathbb{Z}} K_{\alpha_1,\ldots,\alpha_n}\sigma_1^{\alpha_1}\ldots\sigma_1^{\alpha_n}\right) \tag{171}$$

satisfies them also.

If we know just the first two polynomials of the sequence, then the situation is even worse. Kernel solutions on the 3. level will generate descendant polynomials on level 4, where again new kernels can appear, and so on... It shows that the solution of form factor axioms is highly not unique, however we could generate an infinite sequence of solutions which fit well into numerical results.

For further description I separate the ν powers in the polynomials as:

$$Q_n = \nu^{n-1}Q_{n,n-1} + \nu^{n-3}Q_{n,n-3} + \cdots + \nu^{-(n-1)}Q_{n,-(n-1)} \tag{172}$$

It is easy to check, that this is consistent with the recursion relations. In the followings we want to find $Q_{n,\ell}$ polynomials in the general form (168).

The main problem, when we want to find a solution, is the infinite set of parameters in the general formula. However we can use here the following trick: We can characterise the right hand sides of the recursion relations by its asymptotics, when the variables are send to ∞ or 0. Due to both sides are symmetric expressions in x_i variables, the following 4 sets of exponents are enough to characterise their asymptotics.

$$\beta_k(Q) = \lim_{\lambda\to\infty}\frac{\log Q(u, \lambda x_2, \lambda x_3, \ldots, \lambda x_{k+1}, x_{k+2}, \ldots)}{\log\lambda} \tag{173}$$

$$\beta'_k(Q) = \lim_{\lambda\to\infty} \frac{\log Q(\lambda u, \lambda x_2, \lambda x_3, \dots, \lambda x_{k+1}, x_{k+2}, \dots)}{\log \lambda} \tag{174}$$

$$\gamma_k(Q) = \lim_{\lambda\to 0} \frac{\log Q(u, \lambda x_2, \lambda x_3, \dots, \lambda x_{k+1}, x_{k+2}, \dots)}{\log \lambda} \tag{175}$$

$$\gamma'_k(Q) = \lim_{\lambda\to 0} \frac{\log Q(\lambda u, \lambda x_2, \lambda x_3, \dots, \lambda x_{k+1}, x_{k+2}, \dots)}{\log \lambda} \tag{176}$$

Where these exponents are treated as functions, and Q is any expressions with variables $u, x_2, x_3, \dots$

As second step we require that all symmetric polynomials appearing in the sum have to be consistent with this asymptotic behaviour (this is usually not the case in kernel solutions.) We can express this requirement as inequalities:
Dynamical:

$$\sum_{m=1}^{n} \alpha_m \, \beta_k(\sigma_m(u\omega, u\bar{\omega}, x_2, \dots, x_{n-1})) \le \beta_k(C\nu(D_{n-1}(u, x_2, \dots, x_{n-1})Q_{n-1}(u, x_2, \dots, x_{n-1}), \ell)) \tag{177}$$

$$\sum_{m=1}^{n} \alpha_m \, \gamma_k(\sigma_m(u\omega, u\bar{\omega}, x_2, \dots, x_{n-1})) \ge \gamma_k(C\nu(D_{n-1}(u, x_2, \dots, x_{n-1})Q_{n-1}(u, x_2, \dots, x_{n-1}), \ell)) \tag{178}$$

and the same expressions with β'_k and γ'_k.
Kinematical:

$$\sum_{m=1}^{n} \alpha_m \, \beta_k(\sigma_m(u, -u, x_2, \dots, x_{n-1})) \le \beta_k(C\nu(K_{n-2}(u, x_2, \dots, x_{n-1})Q_{n-2}(x_2, \dots, x_{n-1}), \ell)) \tag{179}$$

$$\sum_{m=1}^{n} \alpha_m \, \gamma_k(\sigma_m(u, -u, x_2, \dots, x_{n-1})) \ge \gamma_k(C\nu(K_{n-2}(u, x_2, \dots, x_{n-1})Q_{n-2}(x_2, \dots, x_{n-1}), \ell)) \tag{180}$$

and again the same expressions with β'_k and γ'_k. Where $C\nu(., \ell)$ separates the therm multiplied by ν^ℓ in an expression:

$$C\nu(Q, \ell) = Q_\ell; \qquad Q = \sum_{\ell'} \nu^{\ell'} Q_{\ell'} \tag{181}$$

These inequalities restricted α-s to a finite set $A_\ell = \{\underline{\alpha}\}$. After that, we have to solve the following equations:

$$\begin{aligned} &Q_{n,\ell}((u\omega, u\bar{\omega}, x_2, \dots x_{n-1})) = \\ &\sum_{(\alpha_1,\dots,\alpha_n)\in A_\ell} C^\ell_{\alpha_1,\dots,\alpha_n} \sigma_1^{\alpha_1}(u\omega, u\bar{\omega}, x_2, \dots x_{n-1}) \dots \sigma_n^{\alpha_n}(u\omega, u\bar{\omega}, x_2, \dots x_{n-1}) \\ &= C\nu(D_{n-1}(u, x_2, \dots, x_{n-1})Q_{n-1}(u, x_2, \dots, x_{n-1}), \ell) \end{aligned}$$

$$
\begin{aligned}
&Q_{n,\ell}((u,-u,x_2,\dots x_{n-1})) = \\
&\sum_{(\alpha_1,\dots,\alpha_n)\in A_\ell} C^{\ell}_{\alpha_1,\dots,\alpha_n}\sigma_1^{\alpha_1}(u,-u,x_2,\dots x_{n-1})\dots\sigma_n^{\alpha_n}(u,-u,x_2,\dots x_{n-1}) \\
&= C\nu(K_{n-2}(u,x_2,\dots,x_{n-1})Q_{n-2}(x_2,\dots,x_{n-1}),\ell)
\end{aligned}
$$

These equations can be expand to power series of u and x_i variables, which results an overdetermined set of linear equations in $C^{\ell}_{\alpha_1,\dots,\alpha_n}$.

I could solve these equations uniquely up to level five and construct the polynomials as:

$$
Q_n = \sum_{\ell}\nu^{\ell}\sum_{(\alpha_1,\dots,\alpha_n)\in A_\ell} C^{\ell}_{\alpha_1,\dots,\alpha_n}\sigma_1^{\alpha_1}\sigma_2^{\alpha_2}\dots\sigma_n^{\alpha_n} \tag{182}
$$

The calculated polynomials reads as:

$$
\begin{aligned}
Q_1 &= \sigma_1 && (183)\\
Q_2 &= \bar{\nu}\sigma_1 + \nu\sigma_1\sigma_2 && (184)\\
Q_3 &= \bar{\nu}^2\sigma_1^2 + \sigma_1^2\sigma_2 + \nu^2\sigma_1\sigma_2\sigma_3 && (185)\\
Q_4 &= \bar{\nu}^3\sigma_1^2\sigma_2 + \bar{\nu}\sigma_1^2\sigma_2^2 + \nu\sigma_1\sigma_2^2\sigma_3 + \nu^3\sigma_1\sigma_2\sigma_3\sigma_4 && (186)\\
Q_5 &= \bar{\nu}^4\left(\sigma_1^2\sigma_2\sigma_3 - \sigma_1^2\sigma_5\right) + \bar{\nu}^2\left(\sigma_1^2\sigma_2^2\sigma_3 - \sigma_1^2\sigma_2\sigma_5\right) + && (187)\\
&\quad \left(\sigma_1\sigma_5^2 + \sigma_1\sigma_2^2\sigma_3^2 - 2\sigma_1\sigma_2\sigma_3\sigma_5\right) + \\
&\quad +\nu^2\left(\sigma_1\sigma_2\sigma_3^2\sigma_4 - \sigma_1\sigma_3\sigma_4\sigma_5\right) + \nu^4\left(\sigma_1\sigma_2\sigma_3\sigma_4\sigma_5 - \sigma_1\sigma_4\sigma_5^2\right)
\end{aligned}
$$

Notes: surprisingly the dynamical recursion relations are enough to make the set of variables finite, and to uniquely determine the polynomials. The dynamical recursions are satisfied then automatically.

Using this process theoretically on every level could be found an appropriate polynomial, however the number of needed symbolical calculations incrise rapidly. According to that, we stopped to evaluate polynomials, and together with László Holló we tried to find a pattern in polynomials, to find a closed formula for them.

This pattern finding was inspired by the original work of Zamolodchikov describing the bulk theory [30]. According to that we defined the polynomial P_n as follows:

$$
\begin{aligned}
P_3\left(\{3\}\right) &= 1 && (188)\\
P_4\left(\{4\}\right) &= \sigma_2\left(\{4\}\right) && (189)
\end{aligned}
$$

Let $\Sigma^{(n)}$ be the $(n-3)\times(n-3)$ matrix which is defined as:

$$
\Sigma^{(n)}_{ij}\left(\{n\}\right) = \sigma_{3i-2j+1}\left(\{n\}\right), \tag{190}
$$

and

$$
P_n\left(\{n\}\right) = \det\Sigma^{(n)}. \tag{191}
$$

Where we use the notation: $\{n\} = \{x_1, x_2, \ldots, x_n\}$. These polynomials have the following properties:

$$P_{n+2}(x, -x, \{n\}) = (-1)^{n+1} \frac{1}{2x(\omega - \bar{\omega})} \left(\prod_{i=1}^{n} (x + \omega x_i)(x - \bar{\omega} x_i) - \prod_{i=1}^{n} (x - \omega x_i)(x + \bar{\omega} x_i) \right) P_n(\{n\}) \quad (192)$$

$$P_{n+1}(\omega x, \bar{\omega} x, \{n-1\}) = \prod_{i=1}^{n-1} (x + x_i) P_n(x, \{n-1\}) \quad (193)$$

After that we introduced the S_n Laurent polynomials as

$$Q_n(n) = \sigma_1(n) \sigma_n(n) P_n(n) S_n(n) \quad (194)$$

and derived a much simpler recursive relations:

$$S_{n+1}(\omega x, \bar{\omega} x, n-1) = (\nu x + \bar{\nu} \bar{x}) S_n(x, n-1) \quad (195)$$

$$S_{n+2}(x, -x, n) = -\left(x^2 \nu^2 - 1 + x^{-2} \nu^{-2}\right) S_n(n) \quad (196)$$

These S_ns are Laurent polynomials, which are invariant under the simultaneous change of $x \leftrightarrow x^{-1}$ and $\nu \leftrightarrow \nu^{-1}$. In S_n the coefficient of ν^k is a homogeneous symmetric Laurent-polynomial of degree k, $k \in \{-n+1, -n+3, \ldots, n-1\}$ We could define the following Laurent-polynomials which have these above properties:

$$\tau_k(x_1, \ldots, x_n) = \sum_{\ell=0}^{k} \nu^{2\ell-k} \bar{\sigma}_{k-\ell}(x_1, \ldots, x_n) \sigma_\ell(x_1, \ldots, x_n) \quad (197)$$

We took the ansatz:

$$S_n(n) = \tau_{n-1}(n) - (\tau_{n-5}(n) + \tau_{n-7}(n)) + (\tau_{n-11}(n) + \tau_{n-13}(n)) - \cdots = \\ = \tau_{n-1}(n) + \sum_{m \geq 1} (-1)^m (\tau_{n+1-6m}(n) + \tau_{n-1-6m}(n)) \quad (198)$$

and we could prove that this satisfies the recursive relations and for small n gives back the calculated polynomials. The required identities and the proof can be found in appendix B.

Or final claim is, that the polynomials for operator $\bar{\varphi}$ has the following form:

$$Q_n(n) = \sigma_1(n) \sigma_n(n) P_n(n) S_n(n)$$

With no kernel therms. This claim was investigated numerically using TCSA, and is described in the next subsection.

To determine finite volume elementary form factors for a state labeled by BY quantum numbers, I had to perform the following process:

- I had to determine the rapidities at volume L from Bethe-Yang equations (56)(57);
- Then construct the form factor from equations (45)(47)(48)(49)(50)(161) and (194);
- To get the finite volume corrections, I used equations (59) and (60) for elementary form factors;
- For finite volume diagonal form factors I had to evaluate every parts of equation (64).

7.2 Numerical results

The numerical check of the form factors was made by the TCSA method described in section 5. The program, to build up the Hilbert space and to calculate the matrices in the defect scaling LY case was written by my supervisor, Zoltán Bajnok.

I get the inner product matrix G, and the matrix elements of operators $\hat{\Phi}_+$, $\hat{\Phi}_-$, $\hat{\varphi}$ and $\hat{\bar{\varphi}}$ at *cut*s 8, 10, 12, 14, 16. My task was to build up from these the volume dependent matrix of perturbed Hamiltonian, $H(L, cut)$, to identify as many states as I can, and to calculate the elementary and diagonal form factors of $\bar{\varphi}$. I worked with defect parameter $b = -3 + i\ 0.5$.

From this point the mass is set to 1, so L is now dimensionless.

Here I show the volume dependent energy spectrum of the model, at $cut = 8$, what would be the starting point to identify states, using Bethe-Yang lines.

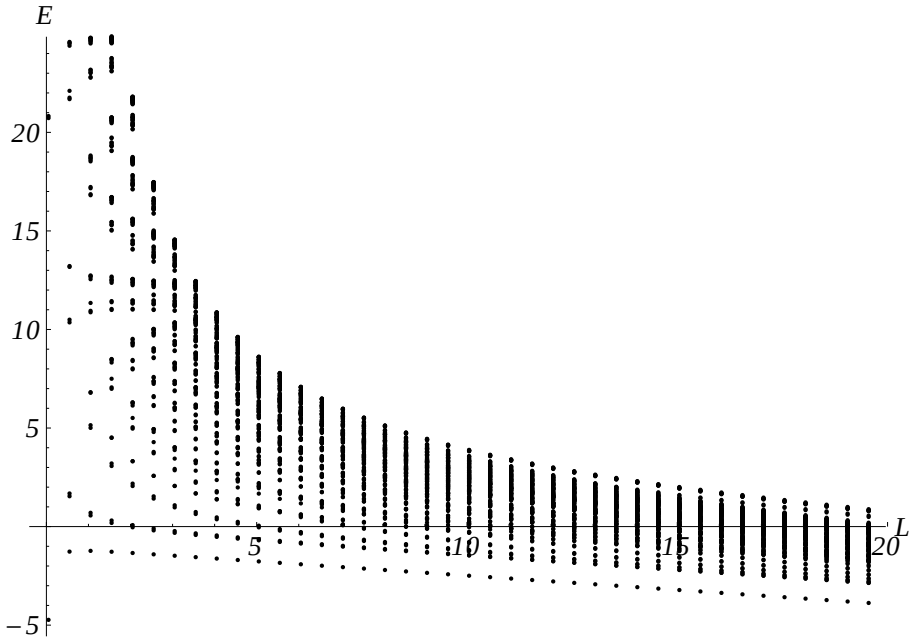

Figure 9: Volume dependent energy spectrum at $cut = 8$

The speciality of this spectrum, is the very near (almost exact) crossings of the energy lines, which is due to integrability. These crosses make hard not just to identify the spectrum points, but also ruins the finding of eigenstates close to the crossing. This is the reason, why data mining from TCSA is so hard.

However in the defect case we have a big luck, because we have an exactly defined operator, the momentum P, which commute with the Hamiltonian, so they have common eigenstates (in the non truncated theory), and for the general value of the defect, the Hilbert space can't be splited to sectors labeled by the momentum.

Because of that, we can introduce a new volume dependent matrix, which is basically the sum of the Hamiltonian and i times the momentum. It will have a volume dependent complex spectrum, where the real part will encode the energy, and the imaginary part the momentum. This trick separates the line crossings, makes the matrix well conditioned,

and makes possible to identify nearly the all states in the spectrum.

To compensate the bulk energy density, and the energy and momentum of the defect, I introduced new operators:

$$H'(L, cut) = H(L, cut) - \varepsilon_B L - \varepsilon_D \tag{199}$$

$$P'(L, cut) = P(L, cut) - p_D \tag{200}$$

Where the defect energy and momentum $\varepsilon_D = \sin(\pi b/6)$, $p_D = -i\cos(\pi b/6)$. The bulk energy density $\varepsilon_B = -1/(4\sqrt{3})$ can be calculated from TBA [29].

To avoid divergences in the UV limit, and to get the energy and the momentum in relative values, I introduced the energy and momentum of one particle calculated from the Bethe-Yang equations, as reference energy and momentum:

$$E_r = \sqrt{1 + \frac{4\pi^2}{L^2}}, \tag{201}$$

$$P_r = \frac{2\pi}{L}, \tag{202}$$

and I introduced the relative Hamiltonian and momentum:

$$H_R(L, cut) = H'(L, cut)/E_r \tag{203}$$

$$P_R(L, cut) = P'(L, cut)/P_r \tag{204}$$

The mentioned composite complex matrix:

$$HiP = H_R + iP_R \tag{205}$$

To see the line structure, and the structure of the complex spectrum at the lowest $cut = 8$, I show here the energy spectrum (in a denser volume spacing), where the colors from blue through black to red encodes the relative momentum of the point.

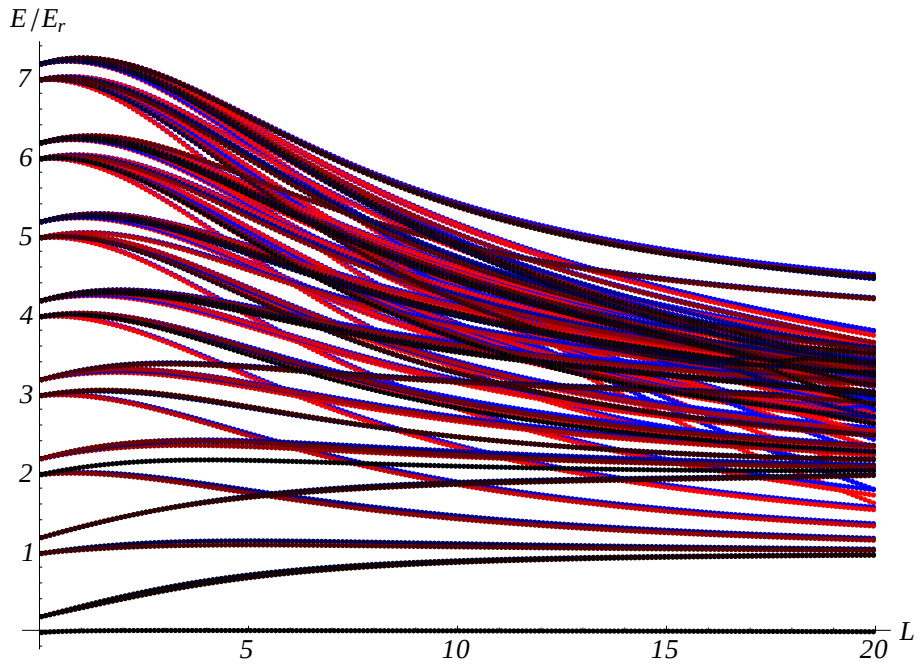

Figure 10: Volume dependent relative energy spectrum at $cut = 8$

To see the complex spectrum structure more transparently, I show it's cross section at volumes $L = 2$ and $L = 10$

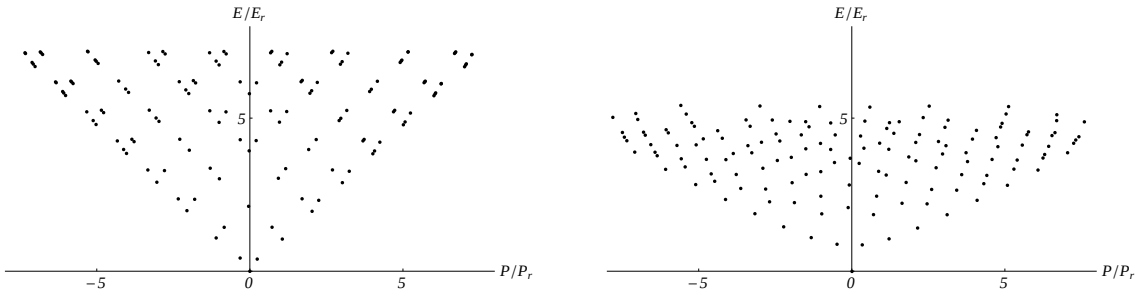

(a) $L = 2$ (b) $L = 10$

Figure 11: Spectrum of HiP at different volumes

After this trick, I could follow a spectrum points and the appropriate state vector under the change of volume on the following way:

At some volume value L_0, I used the `Mathematica` 's built in eigenvector finder, and I choose one state vector V_0. After that I could follow a state vector from volume L_i to $L_i + \Delta L$, by first inverting the matrix $(HiP(L_i + \Delta L) - \lambda_i)$, and then using power iteration to find the closest eigenvector of the new matrix to the previous state vector.

By this method I could identify spectrum points by calculating the BY equations of possible states in the truncated Hilbert space at starting volume $L_0 = 3$, and then follow

them along a wide volume interval (from 0.2 to 20 by steps $\Delta L = 0.2$).

To avoid identification errors at the starting point, in the and of the process I checked if the whole followed line goes with the appropriate BY line.

By this process I could identify 124 states in the TCSA spectrum at $cut = 8$, up to 4 particle states.

This (according to previous results) huge amount of states, makes us possible to prove our assumption on the form factors.

The exact line crossings are typical in integrable theories, because of infinite conserved charges. However if we could identify only one nontrivial conserved charge (which do not split the Hilbert space to distinct sectors, like the momentum in defect less theories), then the same trick could be done.

If we could identify more of them, then the method can be generalized and could result higher numerical stability.

7.2.1 Elementary form factors

After having a list of state vectors, belonging to a chosen state labeled by its BY quantum numbers, it is relatively easy to determine the form factor of a given primary operator at any volume:

$$|\langle 0|O(0)|\underline{n}\rangle_L| = \left| \left(\frac{2\pi}{L}\right)^{h+\bar{h}} \frac{V^\dagger(L,\emptyset)\ O\ V(L,\underline{n})}{\sqrt{V^\dagger(L,\emptyset)\ G\ V(L,\emptyset)}\sqrt{V^\dagger(L,\underline{n})\ G\ V(L,\underline{n})}} \right| \tag{206}$$

Where $V(L,\emptyset)$ belongs to the vacuum state [18], and $\dagger$ means ordinary conjugation and transposition. (The $(2\pi/L)^{h+\bar{h}}$ factor is present, because we have to map back the operator to the cylinder.) For the primary field $\bar{\varphi}$ it is explicitly:

$$|\langle 0|\bar{\varphi}(0)|\underline{n}\rangle_L| = \left| \left(\frac{2\pi}{L}\right)^{1/5} \frac{V^\dagger(L,\emptyset)\ \bar{\varphi}\ V(L,\underline{n})}{\sqrt{V^\dagger(L,\emptyset)\ G\ V(L,\emptyset)}\sqrt{V^\dagger(L,\underline{n})\ G\ V(L,\underline{n})}} \right| \tag{207}$$

For simplicity we do not set the phase of this form factor, so I measured just its absolute value.

I measured the form factors at every volume points mentioned before, for every even cuts between 8 and 16.

After that I used extrapolation at every volume value in the form:

$$FF(L,cut) = A(L) + \frac{B(L)}{cut^\alpha} \tag{208}$$

To get closer to the exact form factor. This extrapolation method was first introduced in [26] for spin less fields, and will be explained for our case in [2]. The exponent α depends on the operator, for what we want to use, but it also depends on the perturbing operators and their OPEs. The calculation will be explained in [2], which results, that the leading therm for $\bar{\varphi}$ in defect scaling LY model is $\alpha = 1$.

[18] here the vacuum means the lowest energy state and will be labeled also as $\emptyset$ or $\{\}$

Now I will show the results, where green points by rising saturation belongs to measured form factors at rising cut levels, black points with error bar belongs to the extrapolated value (error bars show the 95% confidence level of $A(L)$ calculated by `Mathematica`) and continuous red line shoves the theoretical result.

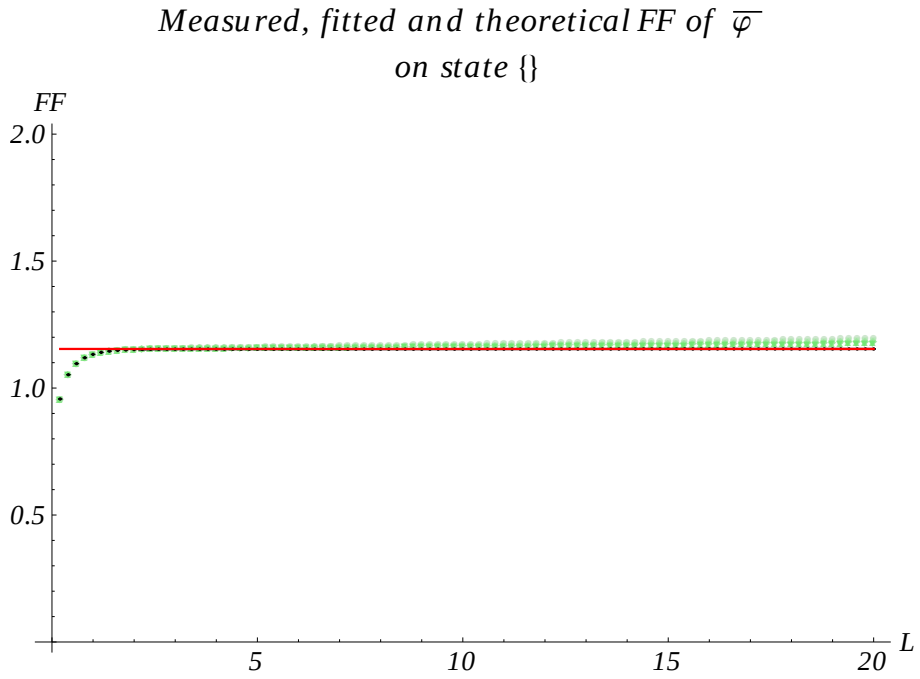

Figure 12: Vacuum expectation value.

It can be seen, that extrapolated data nearly approach the theoretical result, on every domain, where the theory is valid, and the error bars are so small, that they can not be seen on this picture.

To see in one plot the purely measured and extrapolated data, I show the same plot in a finer scale. It will excellently show the accuracy of the energy *cut* extrapolation also:

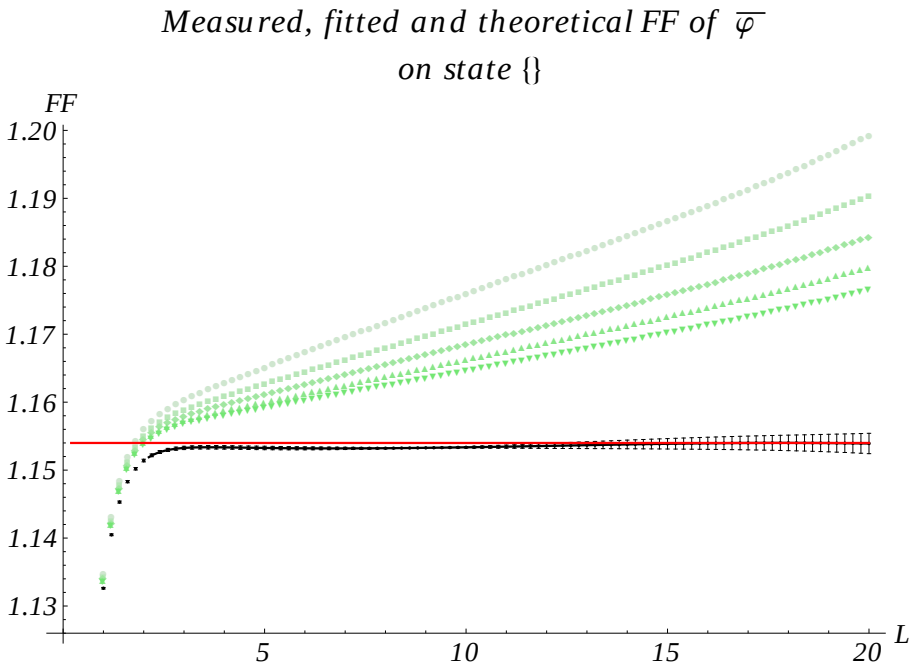

Figure 13: Vacuum expectation value.

To show the absolute accuracy what the extrapolation can achieve, and to motivate its refinements I plot here only the extrapolated and theoretical results in a more finer scale:

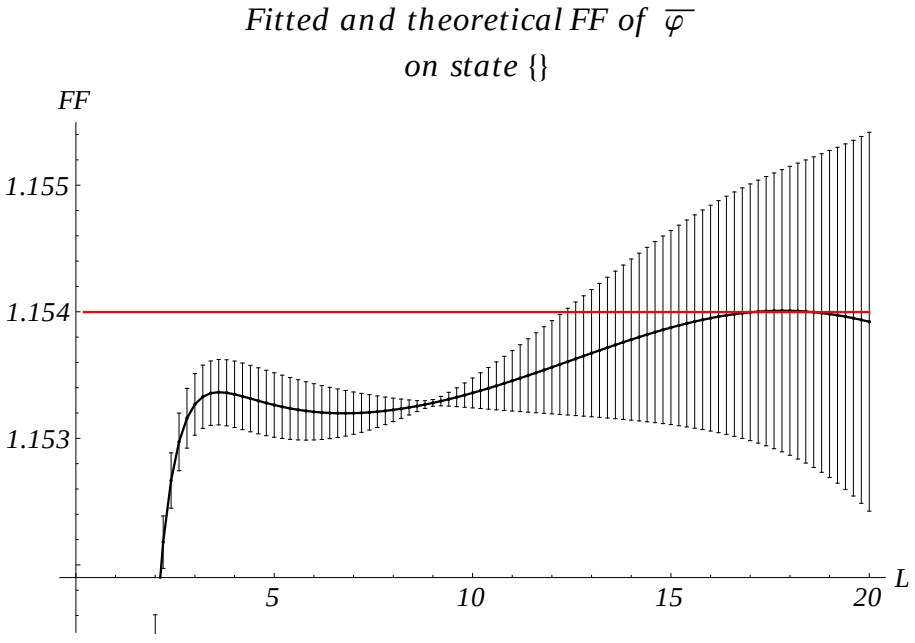

Figure 14: Vacuum expectation value.

Here we can see that an unexpected deviance occurs approximately from $L = 4$ to $L = 12$, which will be discussed later in section 8.

The 3 and 4 particle states identified in the spectrum, gives us the opportunity to directly test our claim on the form factor solutions. I show here a measured 4 particle form factor:

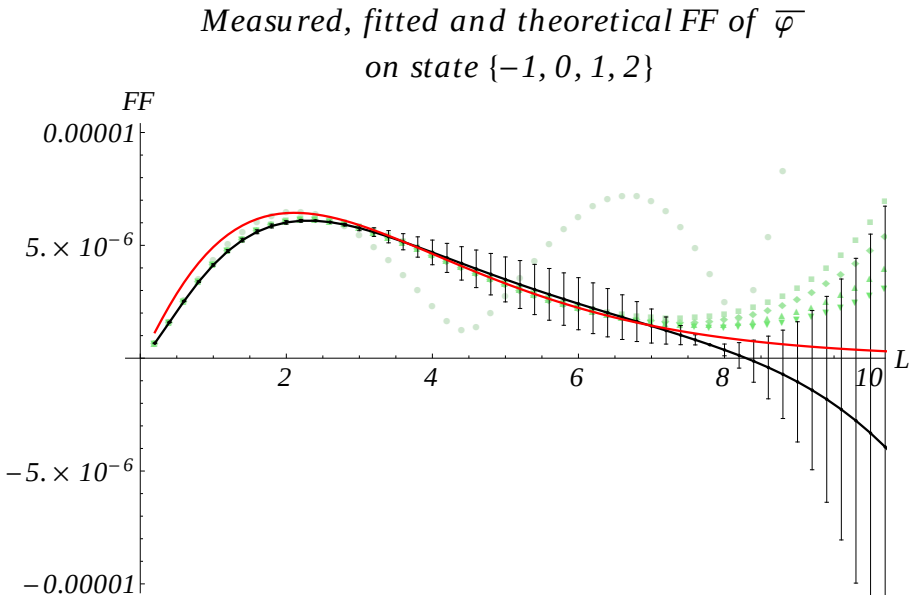

Figure 15: Elementary form factor of 4 particle state

The picture shoves the length interval just up to $L = 10$, because for bigger volumes TCSA data are very unreliable. The fitting process was performed just for the 3 largest *cut* values, because we can see, that for example at lowest $cut = 8$ (represented by green circles) form factor data has huge errors, and it actually oscillates.

However the extrapolated data is suprisingly close to the theoretical predictions, so we can say that the numerical result fits into our theoretical claim.

More measured form factors can be seen in appendix C.

7.2.2 Diagonal form factors

We can measure diagonal form factors of any primary field also:

$$|\langle \underline{n}|O(0)|\underline{n}\rangle_L| = \left| \left(\frac{2\pi}{L}\right)^{h+\bar{h}} \frac{V^\dagger(L,\underline{n})\ O\ V(L,\underline{n})}{V^\dagger(L,\underline{n})\ G\ V(L,\underline{n})} \right| \tag{209}$$

For $\bar{\varphi}$ this reads as:

$$|\langle \underline{n}|\bar{\varphi}(0)|\underline{n}\rangle_L| = \left| \left(\frac{2\pi}{L}\right)^{1/5} \frac{V^\dagger(L,\underline{n})\ \bar{\varphi}(0)\ V(L,\underline{n})}{V^\dagger(L,\underline{n})\ G\ V(L,\underline{n})} \right| \tag{210}$$

To check the coincidence of measured and theoretical diagonal form factors, I had to calculated the connected therms in eq. (64). It was made symbolically by `Mathematica` , but I note, that this was the hardest point of this comparison.

To determine diagonal form factors of an m particle state, we have to use the elementary form factors of $2m$ particle states. This implies, that measuring only two particle diagonal form factors go beyond the theory known before.

To present our best verification of our theoretical claim, I show here a measured extrapolated and calculated 4 particle diagonal form factor. For the analytic calculations 8 particle elementary form factors were needed. This would be practically hopeless without the derived recursive formula for the symmetrical polynomials (194).

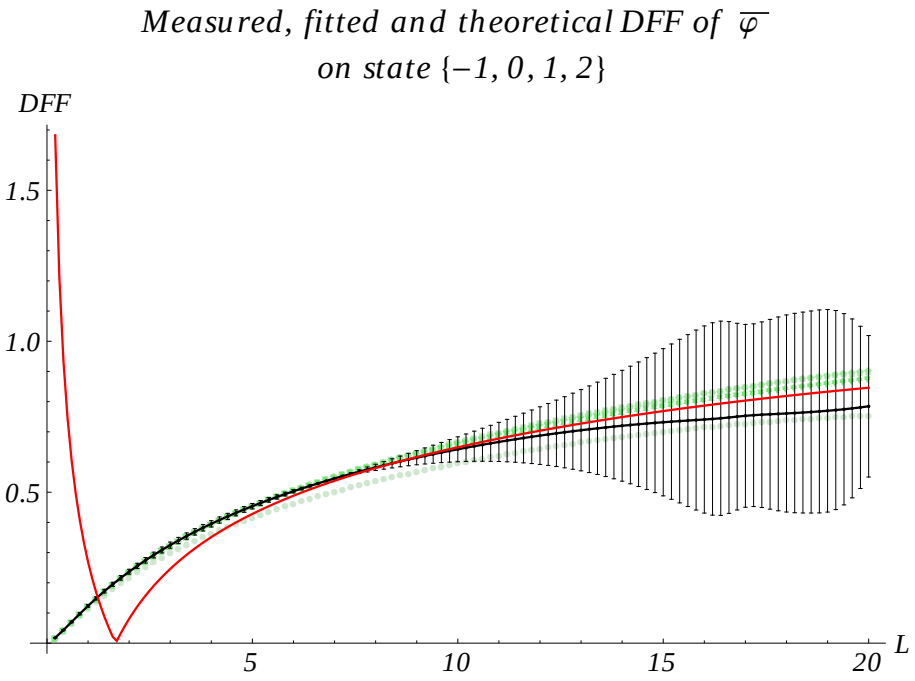

Figure 16: Diagonal form factor of 4 particle state

Due to the unreliability of low *cut* data, the fitting process was performed just for the 3 largest *cut* values.

We can see, that the extrapolated date (black) very well reaches the theoretical results (red) on a very large volume domain up to $L = 20$. At small volumes an exponentional like deviance can be seen, but this shows just the precision limits of finite volume form factor calculations based on the Bethe-Yang equations. (The "reflection" of the theoretical line near to $L = 2$ is just because we took its absolute value.)

More measured diagonal form factors can be seen in appendix C.

Finally I note that numerical and most of the symbolical calculations were made by `Mathematica` .

8 Discussion and future directions

In the present thesis I introduced the main techniques for integrable models, like the S,T-matrix and form factor bootstrap. I presented the simplest finite volume corrections for the form factors provided by the Bethe-Yang equations which contain every polynomial order terms in the inverse volume. As a different treatment of finite volume QFTs I introduced the language of conformal field theory especially in 2D. On this language I was able to fully introduce the defect scaling LY model and the TCSA method.

The main goal of my work was to determine analytically all form factors of the defect operator $\bar{\varphi}$.

It turned out, that the form factor axioms has highly non unique solutions, however I could present a relatively simple formula for the form factor polynomials of any particle number. It can not be said rigorously that the appropriate form factors of $\bar{\varphi}$ has been found, but I used TCSA to numerically check our predictions.

Because of an exact nontrivial momentum known in the defect theory, I could use a new method of state identification in the TCSA spectrum. By this refined method I could identify states up to 4 particles.

To lower the truncation errors, I used the powerful finite *cut* extrapolation. It could serve not just much more accurate data, but by giving an error bar from the fit, it can show the reliability of the method in different volumes.

By measuring 4 particle diagonal form factors, I could test our claim on the form factors up to 8 particles, and I found very good agreement on intermediate volumes.

In this work I measured only the absolute value of the form factors, and the finite *cut* extrapolation was performed on these. However if we prescribe a reality condition for the eigenvectors [2] then we can get complex matrix elements. If we allow for the extrapolation parameters to be complex numbers (what is natural in the framework where the extrapolation method was derived), then we could get more accurate results. This method could decrease the extrapolation errors, when the form factor changes its sign. (What can be seen on figure 20.)

Furthermore we hope, that by this method we can achieve theoretical lines laying inside the error bars in every not too small volumes.

The extrapolation formula gives just the leading order correction in *cut* variable. Due to that low *cut* date are unreliable. This type of errors can be lowered simply by rising the *cut* and make the extrapolations just from the highest *cut* data. In the upcoming paper [2] calculations with $cut = 18$ data will be performed also.

A Structural constants of defect scaling LY model

$$
\begin{aligned}
C^{\mathbb{I}}_{\Phi\Phi} = C^{\mathbb{I}}_{\phi_-\phi_-} = C^{\mathbb{I}}_{\phi_+\phi_+} &= -1 & C^{\mathbb{I}}_{\varphi\varphi} = C^{\mathbb{I}}_{\bar\varphi\bar\varphi} &= -1 \\
C^{\mathbb{I}}_{dd} = C^{\mathbb{I}}_{\bar d\bar d} &= 1 & C^{\mathbb{I}}_{DD} &= -1 \\
C^{\Phi}_{\Phi\Phi} = C^{\phi_-}_{\phi_-\phi_-} = C^{\phi_+}_{\phi_+\phi_+} &= \alpha^2\beta & C^{\varphi}_{\varphi\varphi} = C^{\bar\varphi}_{\bar\varphi\bar\varphi} = C^{D}_{\varphi D} = C^{D}_{\bar\varphi D} &= \alpha\beta^{-1} \\
C^{d}_{\varphi d} = C^{\bar d}_{\bar\varphi\bar d} &= \alpha\beta & & \\
C^{\bar d}_{\varphi D} = C^{d}_{\bar\varphi D} &= 1 & C^{D}_{\varphi\bar d} = C^{D}_{\bar\varphi d} &= -1 \\
C^{\phi_+}_{\varphi\bar\varphi} = C^{\phi_-}_{\bar\varphi\varphi} &= \frac{\beta^{-1}}{1+\eta^{-1}} & C^{\phi_-}_{\varphi\bar\varphi} = C^{\phi_+}_{\bar\varphi\varphi} &= \frac{\beta^{-1}}{1+\eta} \\
C^{D}_{\phi_+ D} = C^{D}_{\phi_- D} &= \alpha^2\beta^{-1} & & \\
C^{d}_{\phi_+ D} = C^{\bar d}_{\phi_- D} &= \alpha\eta & C^{\bar d}_{\phi_+ D} = C^{d}_{\phi_- D} &= \alpha\eta^{-1} \\
C^{d}_{\phi_+\bar d} = C^{\bar d}_{\phi_- d} &= -\eta^2\beta & C^{\bar d}_{\phi_+ d} = C^{d}_{\phi_-\bar d} &= -\eta^{-2}\beta \\
C^{D}_{\phi_+ d} = C^{D}_{\phi_-\bar d} &= -\eta^{-1}\alpha & C^{D}_{\phi_+\bar d} = C^{D}_{\phi_- d} &= -\eta\alpha \\
C^{\mathbb{I}}_{\phi_+\phi_-} = C^{\mathbb{I}}_{\phi_-\phi_+} &= (1+\beta^{-2}) & C^{\phi_+}_{\phi_+\phi_-} = C^{\phi_-}_{\phi_-\phi_+} = C^{\phi_-}_{\phi_+\phi_-} = C^{\phi_+}_{\phi_-\phi_+} &= \beta^{-1}\alpha^2 \\
C^{\varphi}_{\phi_+\phi_-} = C^{\bar\varphi}_{\phi_-\phi_+} &= i\sqrt{\sqrt{5}\,(1+\beta^{-2})} & C^{\bar\varphi}_{\phi_+\phi_-} = C^{\varphi}_{\phi_-\phi_+} &= -i\sqrt{\sqrt{5}\,(1+\beta^{-2})} \\
C^{\varphi}_{\phi_+\bar\varphi} = C^{\bar\varphi}_{\phi_-\varphi} = C^{\varphi}_{\bar\varphi\phi_-} = C^{\bar\varphi}_{\varphi\phi_+} &= -\beta^{-1}\eta & C^{\varphi}_{\bar\varphi\phi_+} = C^{\bar\varphi}_{\varphi\phi_-} = C^{\varphi}_{\phi_-\bar\varphi} = C^{\bar\varphi}_{\phi_+\varphi} &= -\beta^{-1}\eta^{-1} \\
C^{\phi_+}_{\phi_+\varphi} = C^{\phi_-}_{\phi_-\bar\varphi} = C^{\phi_+}_{\bar\varphi\phi_+} = C^{\phi_-}_{\varphi\phi_-} &= \frac{\alpha}{2}\left((\beta+\beta^{-1}) - i\frac{1}{\sqrt[4]{5}}\right) & C^{\phi_+}_{\phi_+\bar\varphi} = C^{\phi_-}_{\phi_-\varphi} = C^{\phi_+}_{\varphi\phi_+} = C^{\phi_-}_{\bar\varphi\phi_-} &= \frac{\alpha}{2}\left((\beta+\beta^{-1}) + i\frac{1}{\sqrt[4]{5}}\right) \\
C^{\phi_+}_{\varphi\phi_-} = C^{\phi_-}_{\bar\varphi\phi_+} = C^{\phi_+}_{\phi_-\bar\varphi} = C^{\phi_-}_{\phi_+\varphi} &= \frac{\alpha\beta}{2}\left(1 + i\,(\beta-\beta^{-1})\,\frac{1}{\sqrt[4]{5}}\right) & C^{\phi_+}_{\bar\varphi\phi_-} = C^{\phi_-}_{\bar\varphi\phi_+} = C^{\phi_+}_{\phi_-\varphi} = C^{\phi_-}_{\phi_+\bar\varphi} &= \frac{\alpha\beta}{2}\left(1 - i\,(\beta-\beta^{-1})\,\frac{1}{\sqrt[4]{5}}\right)
\end{aligned}
$$

where

$$
\alpha = \sqrt{\frac{\Gamma(\frac{1}{5})\Gamma(\frac{6}{5})}{\Gamma(\frac{3}{5})\Gamma(\frac{4}{5})}}\,, \qquad \beta = \sqrt{\frac{2}{1+\sqrt{5}}}\,,
$$
$$
\xi = \mathrm{e}^{i\frac{2\pi}{5}}\,, \qquad \eta = \mathrm{e}^{i\frac{\pi}{5}}\,.
$$

Normalizations of highest weight states

$$
\begin{aligned}
\langle 0|0\rangle &= 1 \\
\langle d|d\rangle = \langle \bar d|\bar d\rangle &= 1 \\
\langle D|D\rangle &= -1
\end{aligned}
$$

B Proof of recursion

We have the fallowing recursion relations for Q_n Laurent polynomials:

$$\begin{aligned} Q_{n+2}(u,-u,u_1,\ldots,u_n) &= K_n(u,u_1,\ldots,u_n)Q_n(u_1,\ldots,u_n) \\ Q_{n+1}(u\omega,u\omega^{-1},u_1,\ldots,u_{n-1}) &= D_n\left(u,u_1,\ldots,u_{n-1}\right)Q_n\left(u,u_1,\ldots,u_{n-1}\right) \end{aligned}$$

with $\omega = e^{\frac{i\pi}{3}} = \bar{\omega}^{-1}$, and

$$\begin{aligned} K_n\left(u,u_1,\ldots,u_n\right) &= (-1)^n \frac{u}{2\left(\omega-\bar{\omega}\right)}\left(u^2\nu^2-1+\bar{u}^2\bar{\nu}^2\right) \\ &\quad \left(\prod_{i=1}^{n}\left(\omega u+\bar{\omega}u_i\right)\left(\bar{\omega}u-\omega u_i\right)-\prod_{i=1}^{n}\left(\omega u-\bar{\omega}u_i\right)\left(\bar{\omega}u+\omega u_i\right)\right) \\ &= (-1)^n \frac{u}{2\left(\omega-\bar{\omega}\right)}\left(u^2\nu^2-1+\bar{u}^2\bar{\nu}^2\right) \\ &\quad \left(\prod_{i=1}^{n}\left(u-\omega u_i\right)\left(u+\bar{\omega}u_i\right)-\prod_{i=1}^{n}\left(u+\omega u_i\right)\left(u-\bar{\omega}u_i\right)\right) \end{aligned}$$

and

$$D_n\left(u,u_1,\ldots,u_{n-1}\right) = \left(\nu u+\bar{\nu}\bar{u}\right)u\left(\prod_{i=1}^{n-1}\left(u+u_i\right)\right)$$

We are going to use the following shorthand notations

$$\{n\} = \{x_1,x_2,\ldots,x_n\}$$

and the elementary symmetric polynomials

$$\prod_{i=1}^{n}\left(x+x_i\right) = \sum_k x^{n-k}\sigma_k\left(\{n\}\right)$$

That also means that if $k>n$ or $k<0$ then $\sigma_k\left(\{n\}\right)=0$. We define

$$\bar{\sigma}_k\left(\{n\}\right) = \sigma_k\left(\frac{1}{x_1},\ldots,\frac{1}{x_n}\right) = \frac{\sigma_{n-k}\left(\{n\}\right)}{\sigma_n\left(\{n\}\right)}$$

Let's introduce the following polynomials from Zamolodchikov's work

$$\begin{aligned} P_3\left(\{3\}\right) &= 1 \\ P_4\left(\{4\}\right) &= \sigma_2\left(\{4\}\right) \end{aligned}$$

Let $\Sigma^{(n)}$ be the $(n-3)\times(n-3)$ matrix which is defined as

$$\Sigma^{(n)}_{ij}\left(\{n\}\right) = \sigma_{3i-2j+1}\left(\{n\}\right)$$

and

$$P_n\left(\{n\}\right) = \det\Sigma^{(n)}$$

These polynomials have the following properties

$$\begin{aligned} P_{n+2}\left(x,-x,\{n\}\right) &= (-1)^{n+1}\frac{1}{2x\left(\omega-\bar{\omega}\right)} \\ &\left(\prod_{i=1}^{n}\left(x+\omega x_i\right)\left(x-\bar{\omega}x_i\right)-\prod_{i=1}^{n}\left(x-\omega x_i\right)\left(x+\bar{\omega}x_i\right)\right)P_n\left(\{n\}\right) \\ P_{n+1}\left(\omega x,\bar{\omega}x,\{n-1\}\right) &= \prod_{i=1}^{n-1}\left(x+x_i\right)P_n\left(x,\{n-1\}\right) \end{aligned}$$

We will use the following identities for the symmetric polynomials:

$$\sigma_k\left(x,x_1,\ldots,x_{n-1}\right) = x\sigma_{k-1}\left(x_1,\ldots,x_{n-1}\right)+\sigma_k\left(x_1,\ldots,x_{n-1}\right) \quad (211)$$

$$\sigma_k\left(\omega x,\bar{\omega}x,x_1,\ldots,x_{n-1}\right) = x^2\sigma_{k-2}\left(x_1,\ldots,x_{n-1}\right)+\sigma_k\left(x,x_1,\ldots,x_{n-1}\right) \quad (212)$$

$$\sigma_k\left(x,-x,x_1,\ldots,x_n\right) = -x^2\sigma_{k-2}\left(x_1,\ldots,x_n\right)+\sigma_k\left(x_1,\ldots,x_n\right) \quad (213)$$

Let's define S_n as

$$Q_n\left(n\right)=\sigma_1\left(n\right)\sigma_n\left(n\right)P_n\left(n\right)S_n\left(n\right)$$

At the dynamical pole

$$\begin{aligned} Q_{n+1}\left(\omega x,\bar{\omega}x,n-1\right) &= \sigma_1\left(\omega x,\bar{\omega}x,n-1\right)\sigma_n\left(\omega x,\bar{\omega}x,n-1\right)P_{n+1}\left(\omega x,\bar{\omega}x,n-1\right)S_{n+1}\left(\omega x,\bar{\omega}x,n-1\right) \\ &= \left(\prod_{i=1}^{n-1}\left(x+x_i\right)\right)\sigma_1\left(x,n-1\right)x\sigma_n\left(x,n-1\right)P_n\left(x,n-1\right)S_{n+1}\left(\omega x,\bar{\omega}x,n-1\right) \end{aligned}$$

The other side of the dynamical recursion relation is

$$\begin{aligned} &\left(\nu x+\bar{\nu}x^{-1}\right)x\left(\prod_{i=1}^{n-1}\left(x+x_i\right)\right)Q_n\left(x,n-1\right)= \\ &\quad=\nu\left(\nu x+\bar{\nu}x^{-1}\right)x\left(\prod_{i=1}^{n-1}\left(x+x_i\right)\right)\sigma_1\left(x,n-1\right)\sigma_n\left(x,n-1\right)P_n\left(x,n-1\right)S_n\left(x,n-1\right) \end{aligned}$$

from that we get

$$S_{n+1}\left(\omega x,\bar{\omega}x,n-1\right)=\left(\nu x+\bar{\nu}\bar{x}\right)S_n\left(x,n-1\right) \quad (214)$$

Similarly at the kinematical pole

$$\begin{aligned} Q_{n+2}\left(x,-x,n\right) &= \nu\sigma_1\left(x,-x,n\right)\sigma_n\left(x,-x,n\right)P_{n+2}\left(x,-x,n\right)S_{n+2}\left(x,-x,n\right)= \\ &= \nu\sigma_1\left(n\right)x^2\sigma_n\left(n\right)(-1)^{n+1}P_n\left(n\right)\frac{1}{2x\left(\omega-\bar{\omega}\right)} \\ &\left(\prod_{i=1}^{n}\left(x+\omega x_i\right)\left(x-\bar{\omega}x_i\right)-\prod_{i=1}^{n}\left(x-\omega x_i\right)\left(x+\bar{\omega}x_i\right)\right)S_{n+2}\left(x,-x,n\right) \end{aligned}$$

and the other side of the kinematical recurrence equation

$$(-1)^n \frac{x}{2(\omega-\bar{\omega})} \left(x^2\nu^2 - 1 + \bar{x}^2\bar{\nu}^2\right) \cdot$$
$$\cdot \left(\prod_{i=1}^n (x-\omega x_i)(x+\bar{\omega}x_i) - \prod_{i=1}^n (x+\omega x_i)(x-\bar{\omega}x_i)\right) \sigma_1(n)\,\sigma_n(n)\,P_n(n)\,Q_n(n)$$

which leads to

$$S_{n+2}(x,-x,n) = -\left(x^2\nu^2 - 1 + x^{-2}\nu^{-2}\right) S_n(n) \tag{215}$$

In case of $\bar{\varphi}$ these S_ns have some general properties as

- As S_3 is invariant for the simultaneous change of $x \leftrightarrow x^{-1}$ $\nu \leftrightarrow \nu^{-1}$, and the recurrence keeps this symmetry, so all of the S_ns have this symmetry
- In S_n the coefficient of ν^k is a homogeneous symmetric Laurent polynomial of degree k, $k \in \{-n+1, -n+3, \ldots, n-1\}$.

The τ_n Laurent polynomials and their properties:

$$\tau_k(x_1,\ldots,x_n) = \sum_{\ell=0}^{k} \nu^{2\ell-k} \bar{\sigma}_{k-\ell}(x_1,\ldots,x_n)\,\sigma_\ell(x_1,\ldots,x_n)$$

They have some important properties what we will use to prove the general form of the form factors of $\bar{\varphi}$.

1. The first such identity is
$$\tau_{n+1}(n) = \tau_{n-1}(n) \tag{216}$$
as
$$\begin{aligned}\tau_{n+1}(n) &= \sum_l \nu^{2l-(n+1)} \underbrace{\bar{\sigma}_{(n+1)-l}}_{\frac{\sigma_{l-1}}{\sigma_n}} \underbrace{\sigma_l}_{\frac{\bar{\sigma}_{n-l}}{\bar{\sigma}_n}} = \sum_l \nu^{2l-(n+1)} \bar{\sigma}_{n-1}\sigma_{l-1} \\ &= \sum_{l'} \nu^{2l'-(n-1)} \bar{\sigma}_{(n-1)-l'}\sigma_{l'} = \tau_{n-1}(n)\end{aligned}$$

2. The second important equation show us the behavior of these τ's at the kinematical pole:
$$\tau_{k+2}(x,-x,n) = \tau_{k+2}(n) + \tau_{k-2}(n) - \left(x^2\nu^2 + x^{-2}\nu^{-2}\right)\tau_k(n) \tag{217}$$
This can be seen as
$$\begin{aligned}\tau_{k+2}(x,-x,n) &= \sum_l \nu^{2l-k-2} \bar{\sigma}_{k+2-l}(x,-x,n)\,\sigma_l(x,-x,n) = \\ &= \sum_l \nu^{2l-k-2} \left(-\frac{1}{x^2}\bar{\sigma}_{k-l}(n) + \bar{\sigma}_{k+2-l}(n)\right)\left(-x^2\sigma_{l-2}(n) + \sigma_l(n)\right) = \\ &= -x^{-2}\sum_l \nu^{2l-k-2}\bar{\sigma}_{k-l}\sigma_l + \sum_l \nu^{2l-(k-2)}\bar{\sigma}_{k-2-l}\sigma_l + \\ &\quad + \sum_l \nu^{2l-(k+2)}\bar{\sigma}_{k+2-l}\sigma_l - x^2\sum_l \nu^{2l-k+2}\bar{\sigma}_{k-l}\sigma_l = \\ &= \tau_{k-2}(n) + \tau_{k+2}(n) - \left(x^2\nu^2 + x^{-2}\nu^{-2}\right)\tau_k(n)\end{aligned}$$

3. We will use this third property to prove the fourth one, this is

$$\tau_k(x,n) = x^{-1}\nu^{-1}\tau_{k-1}(n) + \tau_{k-2}(n) + \tau_k + x\nu\tau_{k-1}(n) \tag{218}$$

as

$$\begin{aligned}
\tau_k(x,n) &= \sum_l \nu^{2l-k}\bar{\sigma}_{k-l}(x,n)\,\sigma_l(x,n) = \\
&= \sum_l \nu^{2l-k}\left(x^{-1}\bar{\sigma}_{k-l-1} + \bar{\sigma}_{k-l}\right)(x\sigma_{l-1} + \sigma_l) = \\
&= x^{-1}\sum_l \nu^{2l-(k-1)-1}\bar{\sigma}_{k-1-l}\sigma_l + \sum_l \nu^{2l-(k-2)}\bar{\sigma}_{k-2-l}\sigma_l + \\
&\quad + \sum_l \nu^{2l-k}\bar{\sigma}_{k-l}\sigma_l + x\sum \nu^{2l-(k-1)+1}\bar{\sigma}_{k-1-l}\sigma_l = \\
&= x^{-1}\nu^{-1}\tau_{k-1} + \tau_{k-2} + \tau_k + x\nu\tau_{k-1}
\end{aligned}$$

4. And finally the behavior of the τ_ns at the dynamical pole is given as

$$\begin{aligned}
\tau_{k+1}\left(x\omega, x\omega^{-1}, n-1\right) &= \left(x^{-1}\nu^{-1} + x\nu\right)\tau_k(x,n-1) - \\
&\quad \tau_{k-1}(n-1) + \tau_{k-3}(n-1) + \tau_{k+1}(n-1)
\end{aligned} \tag{219}$$

which follows from

$$
\begin{aligned}
\tau_{k+1}\left(x\omega,x\bar{\omega},n-1\right) &= \sum_{l}\nu^{2l-k-1}\bar{\sigma}_{k+1-l}\left(x\omega,x\bar{\omega},n-1\right)\sigma_{l}\left(x\omega,x\bar{\omega},n-1\right)\\
&= \sum_{l}\nu^{2l-k-1}\left(x^{-2}\bar{\sigma}_{k-1-l}\left(n-1\right)+\bar{\sigma}_{k+1-l}\left(x,n-1\right)\right)\cdot\\
&\quad \left(x^{2}\sigma_{l-2}\left(n-1\right)+\sigma_{l}\left(x,n-1\right)\right)\\
&= x^{-2}\sum_{l}\nu^{2l-k-1}\bar{\sigma}_{k-1-l}\left(n-1\right)\left(x\sigma_{l-1}\left(n-1\right)+\sigma_{l}\left(n-1\right)\right)+\\
&\quad \sum_{l}\nu^{2l-k-1}\bar{\sigma}_{k-1-l}\left(n-1\right)\sigma_{l-2}\left(n-1\right)+\\
&\quad \sum_{l}\nu^{2l-k-1}\bar{\sigma}_{k+1-l}\left(x,n-1\right)\sigma_{l}\left(x,n-1\right)+\\
&\quad x^{2}\sum_{l}\nu^{2l-k-1}\left(x^{-1}\bar{\sigma}_{k-l}\left(n-1\right)+\bar{\sigma}_{k+1-l}\left(n-1\right)\right)\sigma_{l-2}\left(n-1\right)\\
&= x^{-2}\sum_{l}\nu^{2l-(k-1)-2}\bar{\sigma}_{k-1-l}\left(n-1\right)\sigma_{l}\left(n-1\right)+\\
&\quad x^{-1}\sum_{l}\nu^{2l-(k-2)-1}\bar{\sigma}_{k-2-l}\left(n-1\right)\sigma_{l}\left(n-1\right)+\\
&\quad \sum_{l}\nu^{2l-(k-3)}\bar{\sigma}_{k-3-l}\left(n-1\right)\sigma_{l}\left(n-1\right)+\\
&\quad \sum_{l}\nu^{2l-(k+1)}\bar{\sigma}_{k+1-l}\left(x,n-1\right)\sigma_{l}\left(x,n-1\right)+\\
&\quad x\sum_{l}\nu^{2l-(k-2)+1}\bar{\sigma}_{k-2-l}\left(n-1\right)\sigma_{l}\left(n-1\right)+\\
&\quad x^{2}\sum_{l}\nu^{2l-(k-1)+2}\bar{\sigma}_{k-1-l}\left(n-1\right)\sigma_{l}\left(n-1\right)\\
&= x^{-2}\nu^{-2}\tau_{k-1}\left(n-1\right)+x^{-1}\nu^{-1}\tau_{k-2}\left(n-1\right)+\\
&\quad \tau_{k-3}\left(n-1\right)+x\nu\tau_{k-2}\left(n-1\right)+\\
&\quad +x^{2}\nu^{2}\tau_{k-1}\left(n-1\right)+\tau_{k+1}\left(x,n-1\right)=\\
&= \left(x^{-1}\nu^{-1}+x\nu\right)\tau_{k}\left(x,n-1\right)-\\
&\quad \tau_{k-1}\left(n-1\right)+\tau_{k-3}\left(n-1\right)+\tau_{k+1}\left(n-1\right)
\end{aligned}
$$

where we used the third identity at the last step.

Claim: The following ansatz

$$
\begin{aligned}
S_{n}\left(n\right) &= \tau_{n-1}\left(n\right)-\left(\tau_{n-5}\left(n\right)+\tau_{n-7}\left(n\right)\right)+\left(\tau_{n-11}\left(n\right)+\tau_{n-13}\left(n\right)\right)+\cdots=\\
&= \tau_{n-1}\left(n\right)+\sum_{m\geq1}\left(-1\right)^{m}\left(\tau_{n+1-6m}\left(n\right)+\tau_{n-1-6m}\left(n\right)\right)
\end{aligned}
$$

solves the recurrence relations

Proof:

Kinematical:

With

$$\begin{aligned}\tau_{n+3-6m}(x,-x,n)+\tau_{n+1-6m}(x,-x,n) &= \tau_{n+3-6m}(n)-\left(x^2\nu^2+x^{-2}\nu^{-2}\right)\tau_{n+1-6m}(n)+\\ &\quad \tau_{n-1+6m}(n)+\tau_{n+1-6m}(n)-\\ &\quad \left(x^2\nu^2+x^{-2}\nu^{-2}\right)\tau_{n-1-6m}(n)+\tau_{n-3-6m}(n)\\ &= \tau_{n+3-6m}+\left(1-x^2\nu^2-x^{-2}\nu^{-2}\right)\left(\tau_{n+1-6m}+\tau_{n-1-6m}\right)+\\ &\quad \tau_{n-3-6m}\end{aligned}$$

we get

$$\begin{aligned}S_{n+2}(x,-x,n) &= \tau_{n+1}(x,-x,n)+\sum_{m\geq 1}(-1)^m\left(\tau_{n+3-6m}(x,-x,n)+\tau_{n+1-6m}(x,-x,n)\right)=\\ &= \tau_{n+1}-\left(x^2\nu^2+x^{-2}\nu^{-2}\right)\tau_{n-1}+\tau_{n-3}+\sum_{m\geq 1}(-1)^m\left(\tau_{n+3-6m}+\tau_{n-3-6m}\right)+\\ &\quad +\sum_{m\geq 1}\left(1-x^2\nu^2-x^{-2}\nu^{-2}\right)(-1)^m\left(\tau_{n+1-6m}+\tau_{n-1-6m}\right)=\\ &= \left(1-x^2\nu^2-x^{-2}\nu^{-2}\right)\left(\tau_{n-1}+\sum_{m\geq 1}(-1)^m\left(\tau_{n+1-6m}+\tau_{n-1-6m}\right)\right)=\\ &= \left(1-x^2\nu^2-x^{-2}\nu^{-2}\right)S_n(n)\end{aligned}$$

where in the fourth line we used the first identity for τ.
Dynamical:

$$\begin{aligned}&\tau_{n+2-6m}(x\omega,x\bar{\omega},n-1)+\tau_{n-6m}(x\omega,x\bar{\omega},n-1)=\\ &\quad \tau_{n+2-6m}(n-1)+\left(x^{-1}\nu^{-1}+x\nu\right)\tau_{n+1-6m}(x,n-1)-\tau_{n-6m}(n-1)+\tau_{n-2-6m}(n-1)+\\ &\quad +\tau_{n-6m}(n-1)+\left(x^{-1}\nu^{-1}+x\nu\right)\tau_{n-1-6m}(x,n-1)-\tau_{n-2-6m}(n-1)+\tau_{n-4-6m}(n-1)\\ &= \left(x^{-1}\nu^{-1}+x\nu\right)\left(\tau_{n+1-6m}(x,n-1)+\tau_{n-1-6m}(x,n-1)\right)+\\ &\quad +\tau_{n+2-6m}(n-1)+\tau_{n-4-6m}(n-1)\end{aligned}$$

and finally we get

$$\begin{aligned}S_{n+1}(x\omega,x\bar{\omega},n-1) &= \tau_n(x\omega,x\bar{\omega},n-1)+\\ &\quad \sum_{m\geq 1}(-1)^m\left(\tau_{n+2-6m}(x\omega,x\bar{\omega},n-1)+\tau_{n-6m}(x\omega,x\bar{\omega},n-1)\right)\\ &= \left(x^{-1}\nu^{-1}+x\nu\right)\tau_{n-1}(x,n-1)+\tau_{n-4}(n-1)+\\ &\quad +\sum_{m\geq 1}(-1)^m\left(x^{-1}\nu^{-1}+x\nu\right)\left(\tau_{n+1-6m}(x,n-1)+\tau_{n-1-6m}(x,n-1)\right)+\\ &\quad +\sum_{m\geq 1}(-1)^m\left(\tau_{n+2-6m}(n-1)+\tau_{n-4-6m}(n-1)\right)=\\ &= \left(x^{-1}\nu^{-1}+x\nu\right)\cdot\\ &\quad \left(\tau_{n-1}(x,n-1)+\sum_{m\geq 1}(-1)^m\left(\tau_{n+1-6m}(x,n-1)+\tau_{n-1-6m}(x,n-1)\right)\right)\\ &= \left(x^{-1}\nu^{-1}+x\nu\right)S_n(x,n-1) \qquad \square\end{aligned}$$

C Measured elementary and diagonal form factors of $\bar{\varphi}$

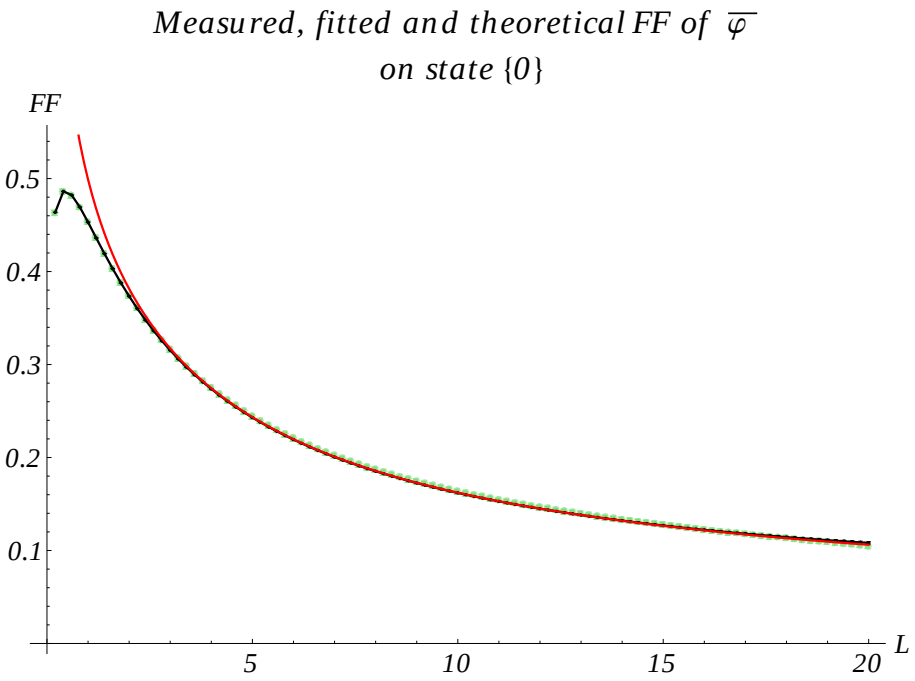

Figure 17: Elementary form factor of 1 particle state

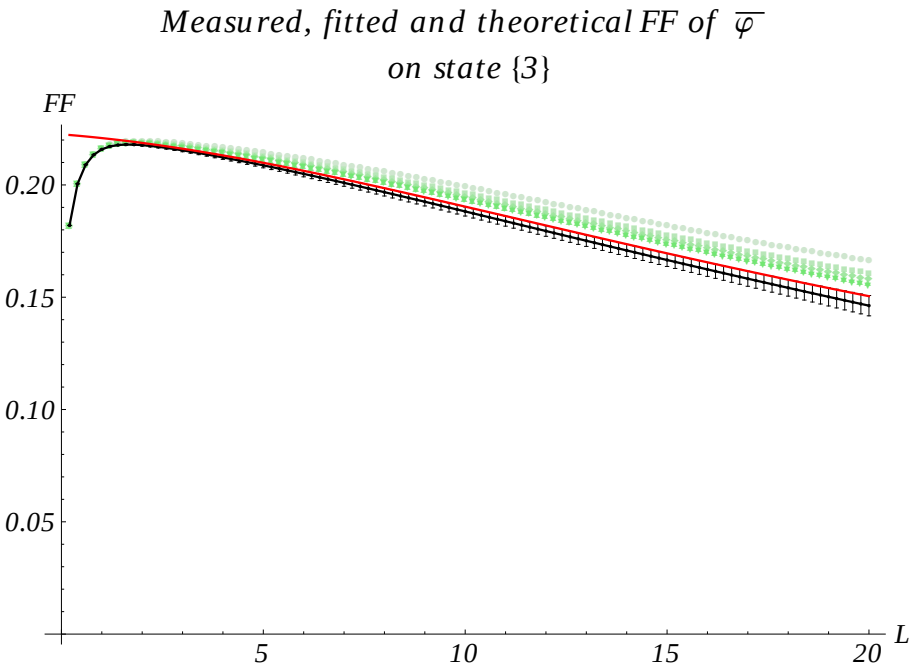

Figure 18: Elementary form factor of 1 particle state

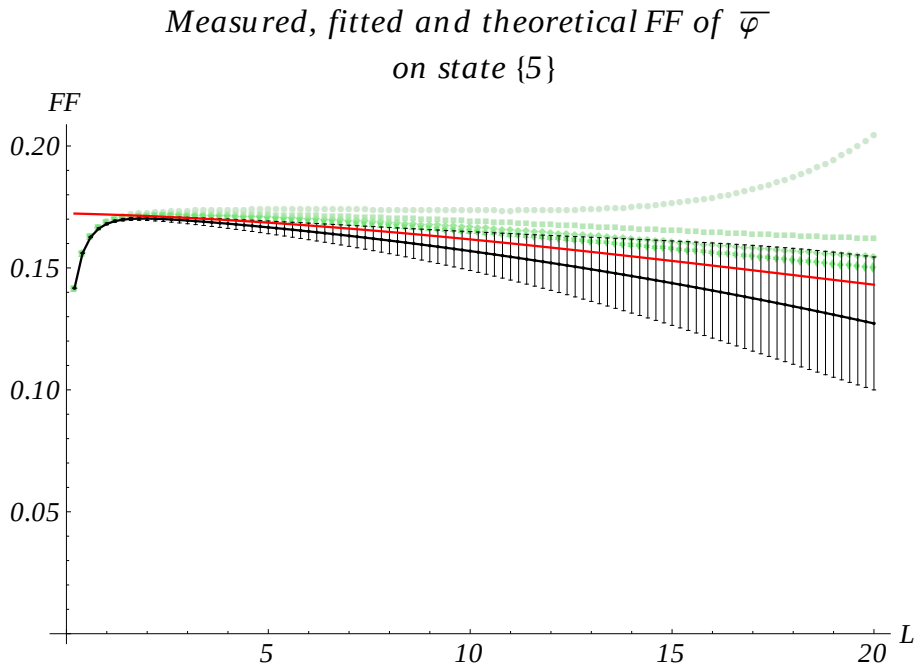

Figure 19: Elementary form factor of 1 particle state

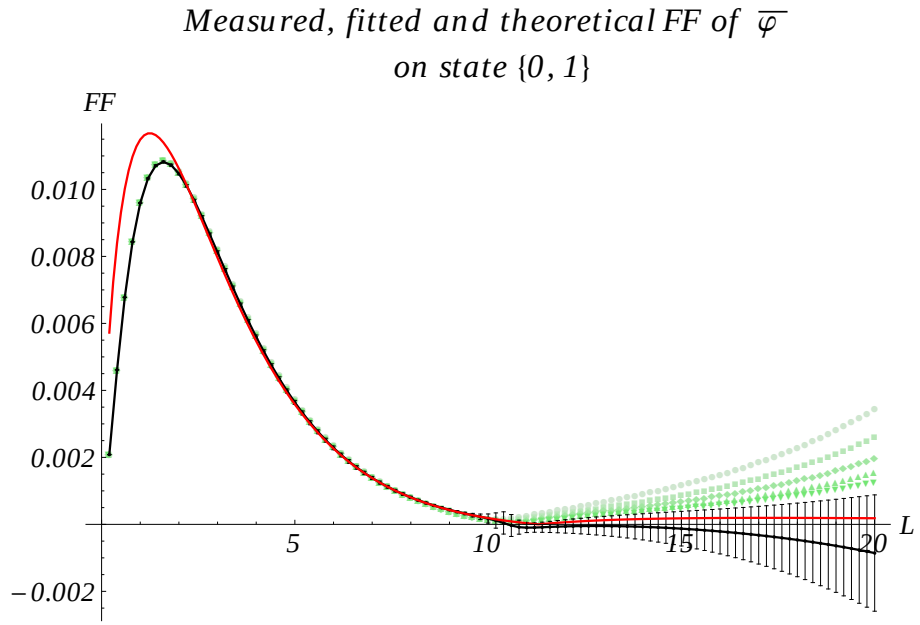

Figure 20: Elementary form factor of 2 particle state

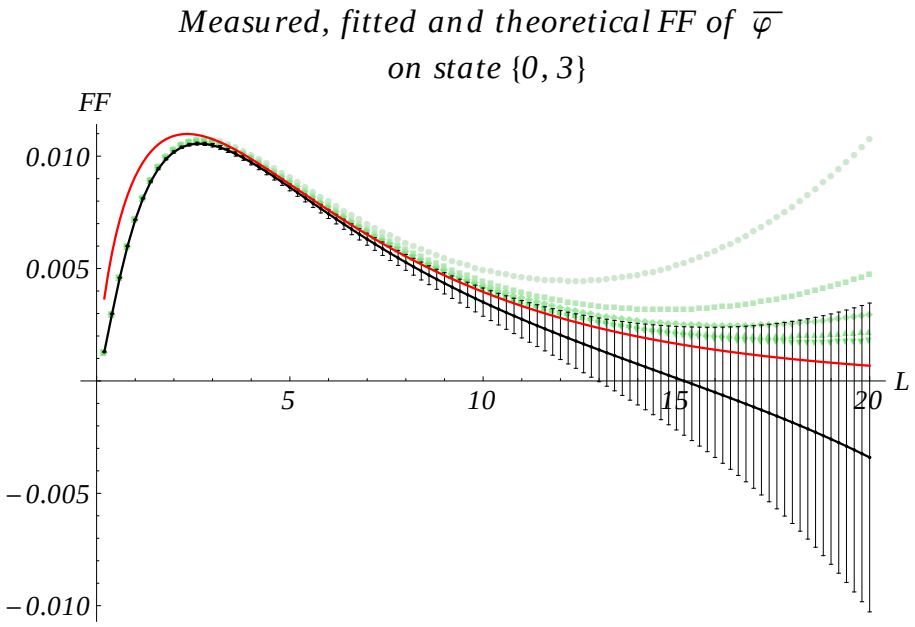

Figure 21: Elementary form factor of 2 particle state

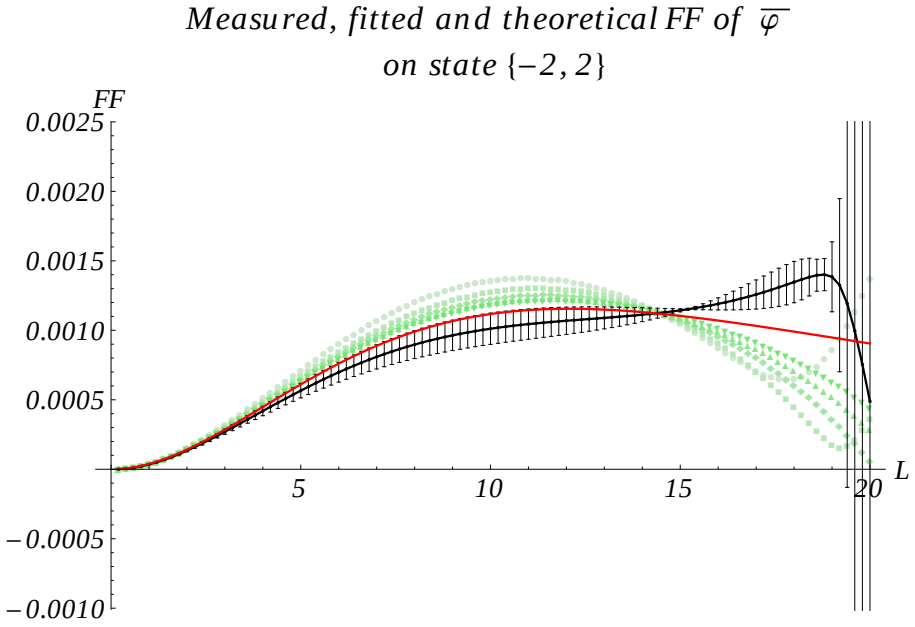

Figure 22: Elementary form factor of 2 particle state

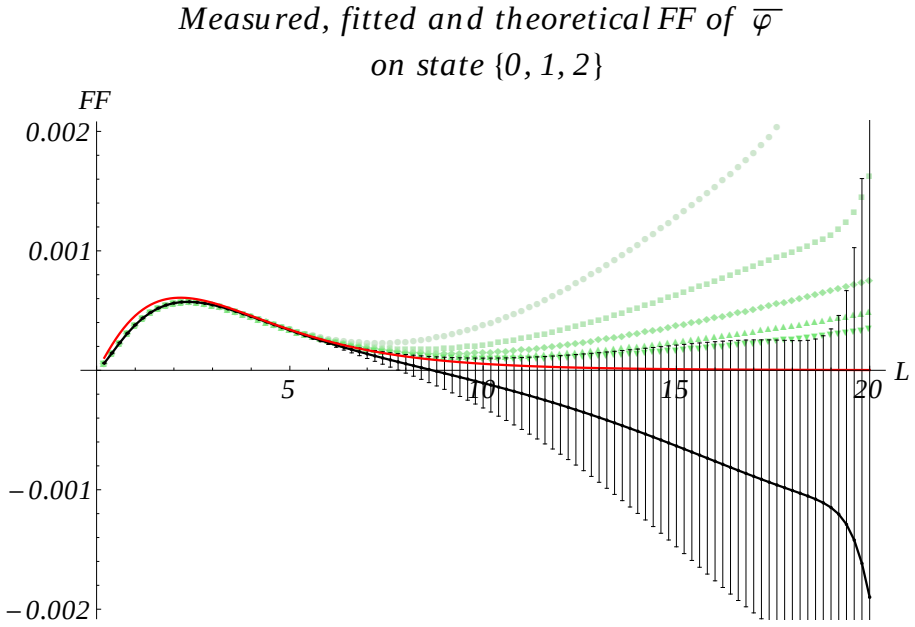

Figure 23: Elementary form factor of 3 particle state

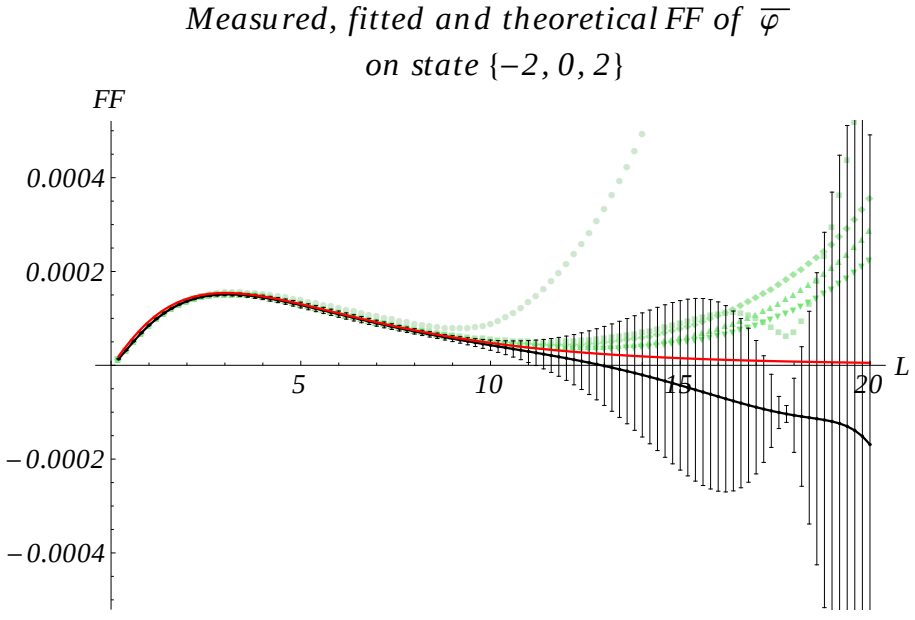

Figure 24: Elementary form factor of 3 particle state

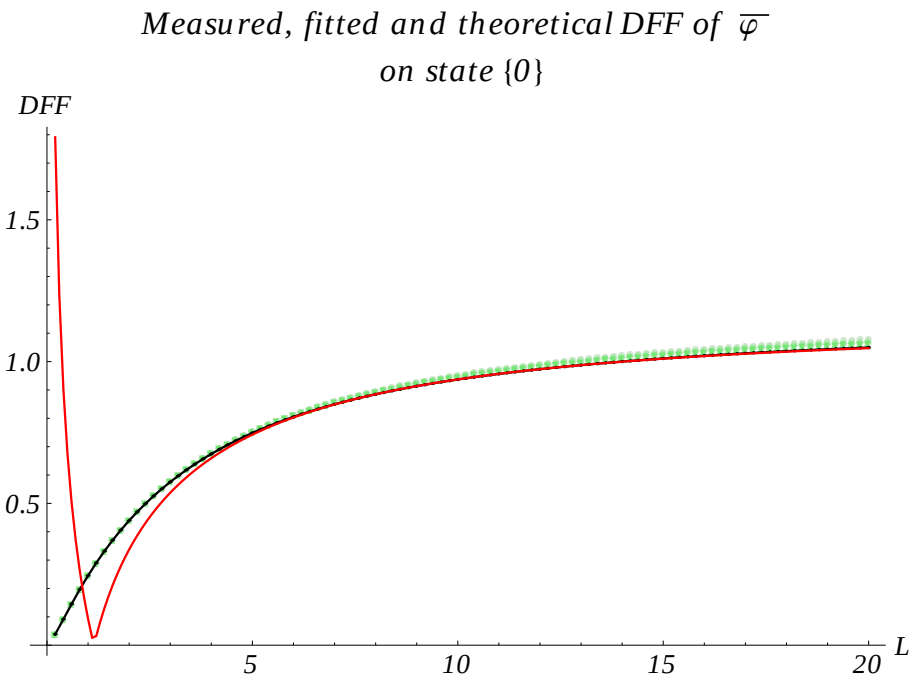

Figure 25: Diagonal form factor of 1 particle state

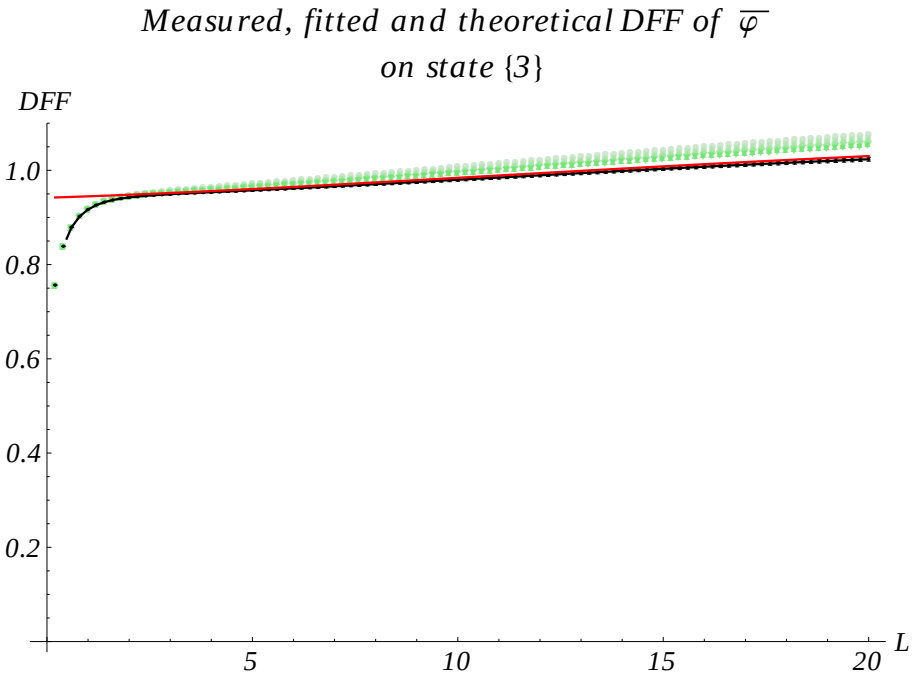

Figure 26: Diagonal form factor of 1 particle state

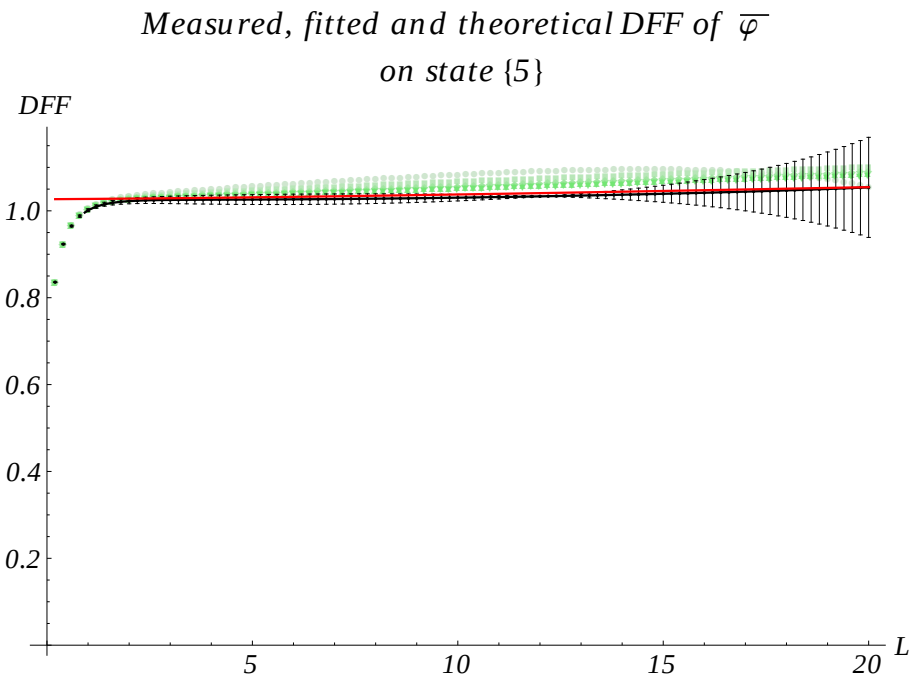

Figure 27: Diagonal form factor of 1 particle state

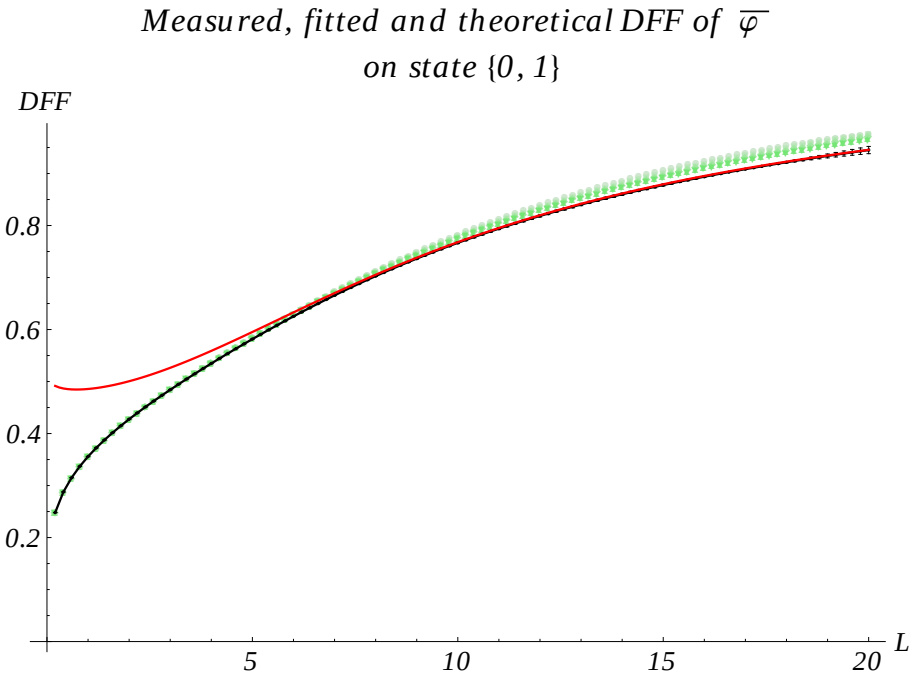

Figure 28: Diagonal form factor of 2 particle state

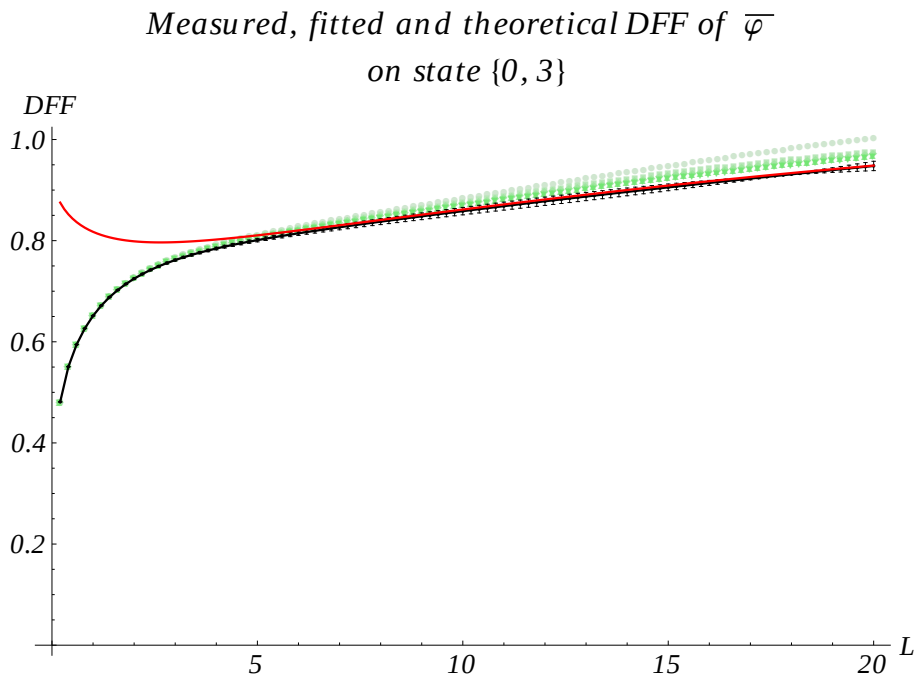

Figure 29: Diagonal form factor of 2 particle state

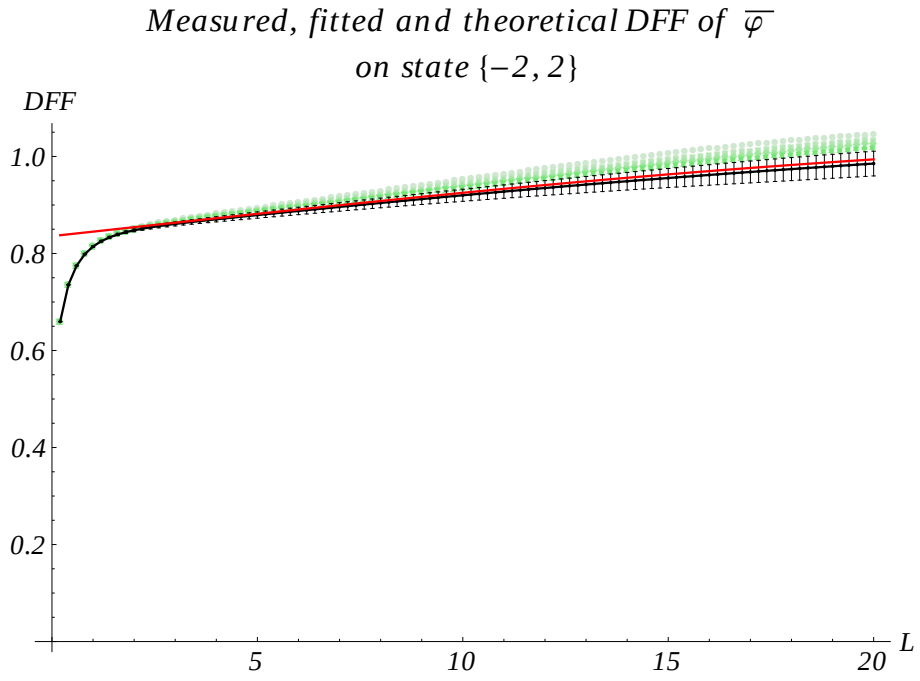

Figure 30: Diagonal form factor of 2 particle state

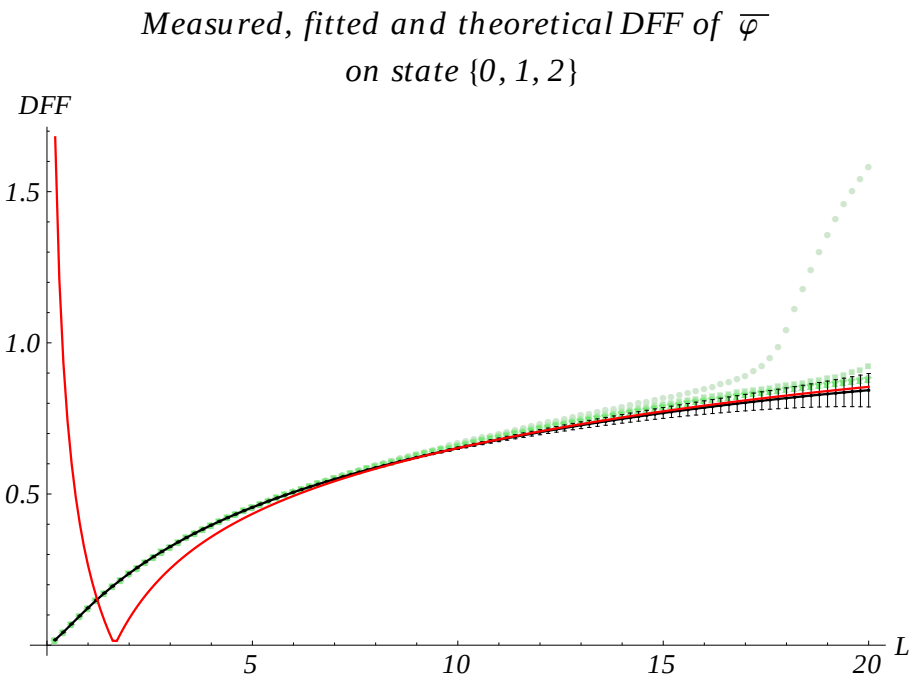

Figure 31: Diagonal form factor of 3 particle state

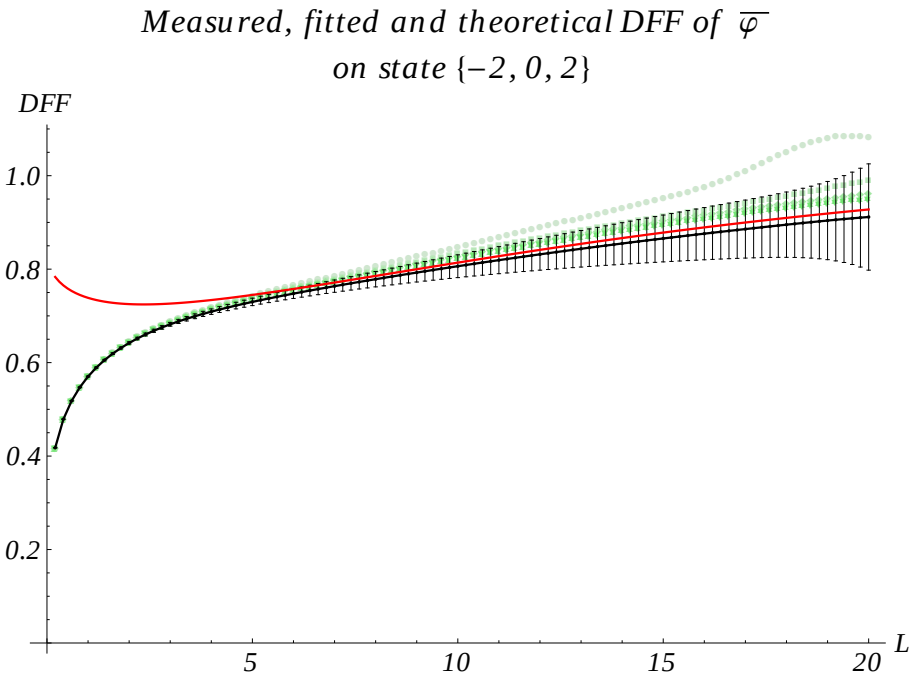

Figure 32: Diagonal form factor of 3 particle state

References

[1] MTA Lendület Holographic Quantum Field Theory Group. http://www.rmki.kfki.hu/~bajnok/Holopage/hqfteng.html. Accessed: 2013-07-10.

[2] Z. Bajnok, F. Buccheri, L. Holló, J. Konczer, and G. Takács. Finite volume form factors in the presence of integrable defects. *Journal of High Energy Physics or Nuclear Physics B*, 2013. In preparation.

[3] Z. Bajnok and O. El Deeb. Form factors in the presence of integrable defects. *Nuclear Physics B*, 832:500–519, June 2010.

[4] Z. Bajnok and A. George. From Defects to Boundaries. *International Journal of Modern Physics A*, 21:1063–1077, 2006.

[5] Z. Bajnok, L. Holló, and G. Watts. Defect scaling Lee-Yang model from the perturbed DCFT point of view. *Journal of High Energy Physics*, 2013. In preparation.

[6] Z. Bajnok, L. Palla, and G. Takács. On the boundary form factor program. *Nuclear Physics B*, 750:179–212, August 2006.

[7] Z. Bajnok and Z. Simon. Solving topological defects via fusion. *Nuclear Physics B*, 802:307–329, October 2008.

[8] Zoltán Bajnok and Ladislav Šamaj. Introduction to integrable many-body systems iii. *Acta Physica Slovaca*, 61(2):129–271, May 2011.

[9] G. Delfino, G. Mussardo, and P. Simonetti. Statistical models with a line of defect. *Physics Letters B*, 328:123–129, May 1994.

[10] Philippe Di Francesco, P. Mathieu, and D. Senechal. *Conformal Field Theory*. Graduate Texts in Contemporary Physics. Springer, 1997.

[11] P. Dorey. Exact S-matrices. *ArXiv High Energy Physics - Theory e-prints*, October 1998.

[12] J.-F. Fortin, B. Grinstein, and A. Stergiou. Scale without conformal invariance: theoretical foundations. *Journal of High Energy Physics*, 7:25, July 2012.

[13] S. Ghoshal and A. Zamolodchikov. Boundary S Matrix and Boundary State in Two-Dimensional Integrable Quantum Field Theory. *International Journal of Modern Physics A*, 9:3841–3885, 1994.

[14] P. Ginsparg. Applied Conformal Field Theory. *ArXiv High Energy Physics - Theory e-prints*, November 1991.

[15] László Holló. Integrálható szennyezések vizsgálata numerikus módszerekkel. Diploma thesis, BME Institute of Physics, Department of Theoretical Physics, 2012.

[16] M. Kormos and G. Takács. Boundary form factors in finite volume. *Nuclear Physics B*, 803:277–298, November 2008.

[17] M. Lüscher. Volume dependence of the energy spectrum in massive quantum field theories. *Communications in Mathematical Physics*, 104(2):177–206, 1986.

[18] M. Lüscher. Volume dependence of the energy spectrum in massive quantum field theories. *Communications in Mathematical Physics*, 105(2):153–188, 1986.

[19] J. Maldacena. The Large-N Limit of Superconformal Field Theories and Supergravity. *International Journal of Theoretical Physics*, 38:1113–1133, 1999.

[20] V. B. Petkova and J.-B. Zuber. Generalised twisted partition functions. *Physics Letters B*, 504:157–164, April 2001.

[21] Joseph Polchinski. Scale and conformal invariance in quantum field theory. *Nuclear Physics B*, 303(2):226 – 236, 1988.

[22] B. Pozsgay and G. Takács. Form factors in finite volume I: Form factor bootstrap and truncated conformal space. *Nuclear Physics B*, 788:167–208, January 2008.

[23] B. Pozsgay and G. Takács. Form factors in finite volume II: Disconnected terms and finite temperature correlators. *Nuclear Physics B*, 788:209–251, January 2008.

[24] L. Šamaj and Z. Bajnok. *Introduction to the Statistical Physics of Integrable Many-body Systems*. Cambridge University Press, 2013.

[25] F.A. Smirnov. *Form Factors in Completely Integrable Models of Quantum Field Theory*. Advanced Series in Mathematical Physics. World Scientific Publishing Company Incorporated, 1992.

[26] I. M. Szécsényi, G. Takács, and G. M. T. Watts. One-point functions in finite volume/temperature: a case study. *ArXiv e-prints*, April 2013.

[27] Gábor Takács. Végesméret effektusok a kvantumtérelméletben. DSc thesis, 2007.

[28] V.P. Yurov and A.B. Zamolodchikov. Truncated conformal space approach to scaling Lee-Yang model. *Int.J.Mod.Phys.*, A5:3221–3246, 1990.

[29] A.B. Zamolodchikov. Thermodynamic Bethe ansatz in relativistic models. scaling three state Potts and Lee-Yang models. *Nucl.Phys.*, B342:695–720, 1990.

[30] Al.B. Zamolodchikov. Two-point correlation function in scaling lee-yang model. *Nuclear Physics B*, 348(3):619 – 641, 1991.

[31] Alexander B Zamolodchikov and Alexey B Zamolodchikov. Factorized S-matrices in two dimensions as the exact solutions of certain relativistic quantum field theory models. *Annals of Physics*, 120(2):253 – 291, 1979.